Calhoun: The NPS Institutional Archive

DSpace Repository

Theses and Dissertations 1. Thesis and Dissertation Collection, all items

1968

Electron Parameagnetic Resonance of the CH2CO2(-) Radical in Irradiated Zinc Acetate Dihydrate.

Crawford, Leslie Paul

Monterey, California. Naval Postgraduate School

http://hdl.handle.net/10945/40058

This publication is a work of the U.S. Government as defined in Title 17, United States Code, Section 101. Copyright protection is not available for this work in the United States.

Downloaded from NPS Archive: Calhoun

Calhoun is the Naval Postgraduate School's public access digital repository for research materials and institutional publications created by the NPS community. Calhoun is named for Professor of Mathematics Guy K. Calhoun, NPS's first appointed -- and published -- scholarly author.

Dudley Knox Library / Naval Postgraduate School
411 Dyer Road / 1 University Circle
Monterey, California USA 93943

http://www.nps.edu/library

UNITED STATES
NAVAL POSTGRADUATE SCHOOL

THESIS

ELECTRON PARAMAGNETIC RESONANCE OF THE $CH_2CO_2^-$ RADICAL IN IRRADIATED ZINC ACETATE DIHYDRATE

by

Leslie Paul Crawford

June 1968

THESIS
C83

[redacted]

[redacted]

ELECTRON PARAMAGNETIC RESONANCE OF THE $CH_2CO_2^-$ RADICAL IN IRRADIATED ZINC ACETATE DIHYDRATE

by

Leslie Paul Crawford
Lieutenant, United States Navy
B.S., University of Arizona, 1962

Submitted in partial fulfillment of the
requirements for the degree of

MASTER OF SCIENCE IN CHEMISTRY

from the

NAVAL POSTGRADUATE SCHOOL
June 1968

Signature of Author Leslie Paul Crawford

Approved by William M. Tolles
Thesis Advisor

G. F. Kinney
Chairman, Department of Chemistry

W. F. Koehler for R. F. Rinehart
Academic Dean

Thesis
C83
c.2

[redacted]

ABSTRACT

An electron paramagnetic resonance study of the $\cdot CH_2CO_2^-$ radical in irradiated zinc acetate dihydrate has been made. The configuration of the radical in the crystalline lattice has been determined as nearly planar using a least squares fit. The HCH angle was found to be 116.9° ± .3°. The principal elements of the α-proton hyperfine tensors were calculated to be: -26.80 ± .74, -59.59 ± .44, -92.15 ± .31 for H_1; -26.41 ± .99, -58.98 ± .45, -92.78 ± .20 for H_2. Three principal values of the g tensor were selected for the best least squares fit: 2.00242, 2.00353, 2.0042. By experiment and an MO calculation the radical has been shown to be a π-electron radical with the unpaired electron localized on the α-carbon. Satellite lines were observed and interpreted as possible "spin-flip" transitions. A temperature dependence of the coupling constants for the 2 protons was discovered from spectra taken at room temperature and at 133°K. Single crystals of $Zn(CH_2DCO_2)_2 \cdot 2H_2O$ were irradiated and an analysis of the spectra showed that the barrier to formation of the radical was the breaking of the C-H bond on the undamaged acetate ion.

DUDLEY KNOX LIBRARY
NAVAL POSTGRADUATE SCHOOL
MONTEREY CA 93943-5101

TABLE OF CONTENTS

	Page
1. ESR Theory - Single Crystal Approach	9
1.1 Review of Radiation Damage Studies	9
1.2 Problem Formulation using Spin Hamiltonian	11
1.3 Solution of the Spin Hamiltonian	14
2. Background on Zinc Acetate Dihydrate	18
3. Experimental	25
3.1 Growing of Crystals	25
3.2 Identification of Crystal Axes	25
3.2.1 X-Ray Diffraction	25
3.2.2 Crystal Alignment	26
3.3 Radiation Dosage	27
3.4 ESR Spectrometer	27
3.5 Synthesis of $Zn(CH_2DCO_2)_2 \cdot 2H_2O$	29
4. Problem Solution and Spectral Analysis	33
4.1 Characterization of the $\cdot CH_2CO_2^-$ radical	33
4.1.1 Theoretical Formulation	33
4.1.2 Data Obtained	38
4.1.3 Correlation of Data with Theory	44
4.1.4 Results	51
4.2 Spectrum of $\cdot CH_2CO_2^-$ radical	54
4.2.1 Observation of the "g-shift"	54
4.2.2 Symmetry of Inequivalent Sites	56
4.2.3 Comparison of Room Temperature Spectra with Low Temperature Spectra	58
4.2.4 Comparison of Calculated and Observed 2nd Order Lines	61

Page

4.2.5 Satellites 63

4.3 Spectrum of Irradiated $Zn(CH_2DCO_2)_2 \cdot 2H_2O$ 67

5. Molecular Orbital Calculation for the $CH_2CO_2^-$ Radical 72

6. Conclusions 74

LIST OF TABLES

Table Page

I Data used for the least squares fit. 39

II Parameters obtained from least squares fit. 53

III Changes in the sum of the coupling constants $(a_{H_1} + a_{H_2})$ for the two methylene protons between room temperature and 133°K. 59

LIST OF ILLUSTRATIONS

Figure Page

1 The orthogonal crystal axis system (xyz or a*bc) and its relationship to the crystalline axis system (abc). 21

2 Locations of the hyperfine axes in the $\cdot CH_2CO_2^-$ radical (planar configuration). 23

3 Single crystal of $Zn(CH_3CO_2)_2 \cdot 2H_2O$ mounted on a quartz rod with the b axis coincident with the axis of the rod. Crystal rotated by ϕ and rod rotated by θ. 28

4 Bending vibrations of the CH_2 group in the $\cdot CH_2CO_2^-$ radical. 32

5 Stereographic net used to catalogue magnetic field orientations. 37

6 Errors in coupling constants for the methylene protons$(\frac{1}{2})$ in $\cdot CH_2CO_2^-$ for a 1° error in angle ϕ. 45

7 ESR spectra of the $\cdot CH_2CO_2^-$ radical at $133^\circ K$. Magnetic field perpendicular to two-fold axis. 47

8 ESR spectra of the $\cdot CH_2CO_2^-$ radical at $133^\circ K$. Magnetic field perpendicular to z axis for $\begin{pmatrix}45\\90\end{pmatrix}$ spectrum and perpendicular to x axis for other spectra. 48

9 ESR spectra of the $\cdot CH_2CO_2^-$ radical at $133^\circ K$ for selected magnetic field orientations. 49

10 ESR spectra of the $\cdot CH_2CO_2^-$ radical at $133^\circ K$. Magnetic field parallel to b axis (top) and perpendicular to z axis in the x-y plane (bottom). Predicted stick spectrum plotted for comparison. 55

11 Comparison of ESR spectra of the $\cdot CH_2CO_2^-$ radical at room (top) and liquid nitrogen (bottom) temperatures with magnetic field parallel to x axis. 57

12 Experimental (E) and predicted (P) spectra of the $\cdot CH_2CO_2^-$ radical showing 2nd order lines. 62

Figure Page

13 ESR spectra of the $\cdot CH_2CO_2^-$ radical. Field direction $\begin{pmatrix}90\\90\end{pmatrix}$ at room temperature. Other spectra at 133°K. 64

14 ESR spectra of $\cdot CH_2CO_2^-$ radical from irradiated single crystals of $Zn(CH_3CO_2)_2 \cdot 2D_2O$ taken at room temperature (top) and 133°K (bottom 2 spectra). 65

15 ESR spectrum of $CHDCO_2^-$ radical with magnetic field perpendicular to b axis. Bottom spectrum predicted assuming a 2:1 ratio of $CHDCO_2^-$: $CH_2CO_2^-$. 68

1. ESR Theory - Single Crystal Approach

1.1 Review of Radiation Damage Studies

Researchers have found that irradiation of certain materials creates one or more paramagnetic species whose study is initially feasible by ESR methods (12). Experiments carried out with polycrystalline samples have unfortunately yielded rather limited information on the hyperfine interactions, i.e., those interactions between nuclei and unpaired electrons. The broadening effect of the resonance lines due to the anisotropy present is known to obscure the weaker signals (4). Single crystals offer the best means of characterizing these hyperfine splittings in that radicals produced by irradiation of single crystals have well-defined orientations in the crystal lattice. The external magnetic field can then be located with respect to the radical.

Since the first application of ESR Spectroscopy in radiation damage studies about 14 years ago, work with single crystals have included in part the saturated dicarboxylic acids and their salts, the simpler amino acids, and certain unsaturated acids (6). The radical may be generated by irradiation at room temperature or low temperatures and stability may be dependent on such factors as the environment in which the radical was created. Furthermore a radical generated by low temperature irradiation does not necessarily mean that subsequent warm up will result in detection of the radical produced by room temperature irradiation. The study of two radicals in irradiated crystals may be enhanced by the fact that although both radicals are generated at room temperature, only one of the radicals is present after low temperature irradiation.

Once a radical is generated in a known crystal lattice ESR techniques can extract important information about the radical. The measurement of the anisotropic hyperfine interactions in the experimental spectra leads to the determination of one or more coupling tensors. The coupling tensor of the radical $\cdot CH(CO_2H)_2$ in irradiated malonic acid was obtained from measurements of the splittings of resonance lines at various magnetic field orientations (11). The tensor's principal values,which are located along an orthogonal set of molecular axes in the radical, are related to the coupling tensor by a similarity transformation. Thus the orientation of the radical in the crystal lattice with respect to the molecular axis system is partially known. The g tensor can be obtained by comparing the radical's hyperfine splittings with those of a standard whose ESR spectrum is observed at the same time. The N^{14} splittings of the three lines of peroxylamine disulfonate in aqueous solution are used for such purposes (14). It should be mentioned that ESR studies of single crystals at controlled temperatures, after irradiation at low temperatures, can yield important information about radiation damage processes. For further discussion of ESR methods in radiation damage studies Morton has an excellent review on the subject (12).

1.2 Problem Formulation using Spin Hamiltonian

In dealing with a free radical in which a single unpaired electron may interact with several nuclei the effective spin Hamiltonian (using the notation of Slichter) is

$$\mathcal{H} = \beta \vec{H}\cdot\vec{\vec{g}}\cdot\vec{S} - \sum_i \gamma_i \hbar \vec{H}\cdot\vec{I}_i + \sum_i \vec{S}\cdot\vec{\vec{A}}_i\cdot\vec{I}_i \tag{21}$$

This expression describes the interaction of nuclei and an unpaired electron in an external magnetic field for the case of quenched orbital angular momentum. The first term represents the Zeeman energy, the energy of interaction of the electron spin moment with the external magnetic field. β is the Bohr magneton; $\vec{S}$ is the electronic spin; and $\vec{\vec{g}}$ is the spectroscopic splitting tensor. The second term is a summation of the Zeeman energies of the nuclei where $\vec{I}_i$ is the spin of the ith nucleus and γ_i is the gyromagnetic ratio of the ith nucleus. The third term represents the summation of the energy of the hyperfine interaction between the electronic spin $\vec{S}$ and the spin of the ith nucleus $\vec{I}_i$. $\vec{\vec{A}}_i$ is the hyperfine interaction tensor. The last term is better known as the combined effect of the isotropic Fermi contact interaction and the anisotropic dipolar interaction.

To obtain information about the A and g tensors experimental measurements must be made on a single crystal in which the radical in this case has been formed by irradiation. From the outward appearance of the crystal a set of orthogonal axes can be chosen (x, y, z) and the crystal can then be rotated with knowledge of the position of the external magnetic field with respect to these axes. It is possible to derive values of the elements of the A tensor in terms of the x, y, z system of axes (3). The transformation which diagonalizes this tensor will then define the relative orientation of the x, y, z system with respect to the radical principal orthogonal axes (X, Y, Z). But one cannot determine from the ESR spectrum alone which of the principal axes is X, Y, or Z. If the crystal structure of the molecule is known and it is assumed that the orientation of the atoms in the radical does not differ with that of the undamaged molecule, then these principal axes can be assigned. The investigation of the radical $HCNH_3^+CO_2^-$ in irradiated glycine by Ghosh and Whiffen was greatly enhanced by the known crystal structure of glycine (8). As in most radicals of this type the carboxyl group in the undamaged glycine is assumed to be unmoved following irradiation (2). This is not an unlikely possibility and is a good basis on which to begin calculations of the direction cosines of the radical's principal axes with respect to the crystal axis system. These are the direction cosines that would be obtained from diagonalizing the A tensor. The principal values of the A tensor will lie along the principal axes in the radical. For the case of an α-proton coupling tensor the smallest value of the diagonal tensor corresponds to the direction of the C-H bond. Thus when the external magnetic field is placed along the C-H bond the interaction between the dipoles of the electron and nucleus is a minimum. If there are two nuclei with which the single unpaired electron can interact then there will exist 2 sets of principal axes, one for each coupling tensor.

The g tensor is anisotropic when the electron possesses both spin and orbital angular momentum (3). Thus in the electronic Zeeman interaction

$$\mathcal{H} = \beta \vec{H} \cdot \overset{\rightrightarrows}{g} \cdot \vec{S}$$

$\vec{S}$ does not represent the true spin of the electron since g tensors are anisotropic because the spin is not oriented exactly along the field direction. The true Hamiltonian for the magnetic interaction is

$$\mathcal{H} = \beta \vec{H} \cdot \vec{L} + g_e \beta \vec{H} \cdot \vec{S}$$

where $\vec{L}$ is the orbital angular momentum. The effects of this perturbing Hamiltonian may be represented by an "effective spin Hamiltonian" where S is considered as a fictitious spin. An accepted treatment is as follows:

$$\mathcal{H} = \vec{H}_{eff} \cdot \vec{S}$$

$$\vec{H}_{eff} = \vec{H} \cdot \overset{\rightrightarrows}{g} = Hg' \vec{h}$$

Now the electron spin will be quantized along the unit vector $\vec{h}$ where Hg' is the magnitude of H_{eff} and g' describes the effective magnetic moment of the molecule. Using the 3 principal values of the g tensor (g_{xx}, g_{yy}, g_{zz}) and the direction cosines of the magnetic field in the principal axis system $(\alpha_x, \alpha_y, \alpha_z)$.

$$g' = \left(g_{xx}^2 \alpha_x^2 + g_{yy}^2 \alpha_y^2 + g_{zz}^2 \alpha_z^2\right)^{\frac{1}{2}}$$

The principal axes of the g tensor will not necessarily coincide with those of the hyperfine tensor.

Once the g and A tensors are known the effective spin Hamiltonian can be used to calculate the probable transitions that will occur and thus the spectrum for a particular orientation of the external magnetic field can be predicted.

1.3 Solution of the Spin Hamiltonian

With the A and g tensors for a particular molecule, a method must be used to obtain the transition frequencies and their probabilities between various energy levels in the molecule. One such method can be outlined as follows:

a. Consider the interaction of a single unpaired electron with n nuclei and form the basis functions to be used in setting up the Hermitian matrix. The basis functions will be of the form

$$|m_s m_{I_1} m_{I_2} \cdots\cdots m_{I_n}\rangle$$

i.e., the product of the electron spin function and n nuclear spin functions. The matrix will be a square matrix with 2^x elements on a side where x = number of spin functions.

b. Operate on the terms in the effective spin Hamiltonian with all required permutations of the basis functions. The diagonal elements are

$$\langle m_s m_{I_1} \cdots m_{I_n} | \mathcal{H} | m_s m_{I_1} \cdots m_{I_n}\rangle = g\beta H_0 m_s + \sum_i A_{zz}^{(i)} m_s m_{I(i)} + \sum_i \gamma_i H_0 m_{I(i)}$$

The off diagonal elements will contain imaginary elements due to the Hermitian properties of the system. The Hermitian matrix can be diagonalized by a method described by Wilkinson (33). Using this method a real matrix is created and the resulting eigenvalues and eigenvectors occur in pairs.

c. Set up the transition probability matrix and transpose to the diagonal basis. Since the eigenvectors are imaginary the transformation can be handled as follows:

Eigenvector = $U + iV$

Transition probability matrix = P

$$P' = (U+iV)P(U-iV)' = UPU' + VAV' + i(VPU' - UPV')$$

d. Square the elements of the transition probability matrix in the diagonal basis. The absolute value of P_{ij} squared is the relative intensity of the transition occurring at frequency $\lambda_j - \lambda_i$. The λ's are the eigenvalues expressed in megacycles. With frequencies and intensities the spectral envelope can be drawn using the derivative of a Lorentzian distribution.

The following alternative solution of the Spin Hamiltonian was used by Box (2) in his treatment of deuterated glycine, $^{+}ND_3CH_2COO^{-}$. The effective spin Hamiltonian is the same as described in section 1.2. By ignoring the components of $\vec{S}$ perpendicular to $\vec{H}$ the energy levels of the spin system are given by

$$E = \beta g H S_H - g_n \beta_n \sum_i I_{ih} |\vec{h}_i|$$

where g is the observed g value, S_H is the component of $\vec{S}$ along $\vec{H}$, and I_{ih} is the component of $\vec{I}_i$ along $\vec{h}_i$ where $\vec{h}_i$ is defined by the equation

$$\vec{h}_i = \vec{H} - S_H \left(\vec{u}_i A \alpha_i + \vec{v}_i B \beta_i + \vec{w}_i C \gamma_i\right) \frac{1}{g_n \beta_n}$$

A, B and C are the principal values of the hyperfine tensor, $\overset{\rightrightarrows}{A}_i$. The unit vectors $\vec{u}_i$, $\vec{v}_i$, $\vec{w}_i$ are the vectors along which each of the principal values A, B, and C lie in the crystal axis system. The direction cosines of the external field with respect to the crystal axes are given by α_i, β_i, γ_i. The relative probabilities of the transitions are functions of the angle between the vectors $\vec{h}_i$ (+) and $\vec{h}_i$ (-), the values of $\vec{h}_i$ corresponding to S_H equal to $+\frac{1}{2}$ and $-\frac{1}{2}$, respectively.

A computer program was developed using the above theory to calculate the relative intensities and frequencies for the transitions which occur (23). Interactions are considered between a single unpaired electron and any number of nuclei. However, the orientation of the radical in the crystal must be known in order to calculate the vectors $\vec{h}_i$ (+) and $\vec{h}_i$ (-). The unit vectors

$\vec{u}_i$, $\vec{v}_i$, $\vec{w}_i$ are the direction cosines which place the principal values of the A tensor along the crystal axes. The program, shown in Appendix I, does not calculate the g anisotropic effect but assumes $g = 2.0023$. Hereafter, this program shall be referred to as PREDICT.

2. Background on Zinc Acetate Dihydrate

Many investigations have been focused on the hyperfine interaction between α- protons and a single unpaired electron in the 2 p_z - orbital of the central carbon atom for radicals such as $HC-(COOH)_2$ (11). In many of the systems studied several π-electron radicals were created by irradiation thus making identification of spectra difficult. The $\cdot CH_2CO_2^-$ radical has been observed with the $NH_3^+CH_2CO_2^-$ radical in irradiated glycine (13). In working with the glycine single crystals, Morton concluded that the two α-proton coupling tensors of $\cdot CH_2COO^-$ have axial symmetry and suggested that the CH_2 group was experiencing hindered rotation about the C-C bond. Box and Freund demonstrated an application of ESR theory to the radical in irradiated glycine and had success in assuming the radical was planar. Horsfield and co-workers showed that for the $\cdot CH_2CO_2H$ radical in malonic acid, the plane of the CH_2 group was approximately perpendicular to the plane of the (CO_2H) group. A value of $116.5^\circ \pm 5^\circ$ was obtained for the HCH angle in the $\cdot CH_2CO_2H$ radical (9). The principal values of the 2 coupling tensors obtained for this radical were

H_1	H_2
-30	-37
-55	-59
-91	-92

Morton calculated for the $CH_2CO_2^-$ radical (planar) the following principal values for the coupling tensors, assuming the tensors to be equivalent (13).

H_1 and H_2

-48

-56

-69

But Box and Freund successfully predicted a spectra for the planar $\cdot CH_2CO_2^-$ in glycine by using the principal values of the coupling tensor obtained by McConnell (11) for $\cdot CH(COOH)_2$.

-29

-61

-91

Valenti discovered that the $CH_2CO_2^-$ radical existed in irradiated Zinc Acetate Dihydrate (28). The radical was found to be stable at room and liquid nitrogen temperatures. The spectra taken as the temperature was lowered showed the center line of the 1:2:1 hyperfine pattern splitting into 2 lines. This confirmed previous observations that a barrier to internal rotation must exist (13). The use of 1st order perturbation theory yielded the principal values of the two α-proton coupling tensors but the spectra was too complex for any further analysis with this theory. This was the motivation for a complete investigation of the $CH_2CO_2^-$ radical, but specifically: (a) to explain the suspected anistropic effects in the complex spectra for various orientations of the external magnetic field; (b) to predict by a theoretical calculation the exact spectra of the $CH_2CO_2^-$ radical; (c) to obtain not only the best principal values of the A and g tensors but the correct orientation of the radical in the crystal within the error limits of a least squares fit; and (d) then to prepare $Zn(CH_2DCO_2)_2 \cdot 2H_2O$ crystals for exchange rate and barrier studies.

The orientation of the radical in the crystal was calculated by starting with the information given by van Niekirk, et. al (18). The crystal structure of $Zn(CH_2CO_2)_2 \cdot 2H_2O$ is monoclinic with space group C 2/c and unit cell dimensions of a = 14.5, b = 5.32, c = 11.02 angstroms with $\beta = 100^\circ$ (Figure 1). The Zn atoms lie on a 2-fold axis and although there are 4 formula units per unit cell, only two magnetically inequivalent sites exist. The relationship of the orthogonal axis system to the cell axis system is

$$a = \sin\beta\, x + \cos\beta\, z$$

$$b = y$$

$$c = z$$

X will also be referred to as a*. With these relationships the coordinates of the atoms in the x, y, z system were calculated to be

	x	y	z
Zn	0.0	.665	2.755
O_1	1.014	1.064	.868
O_2	1.471	2.250	2.683
C_1	1.613	2.128	1.314
C_2	2.614	2.804	.454

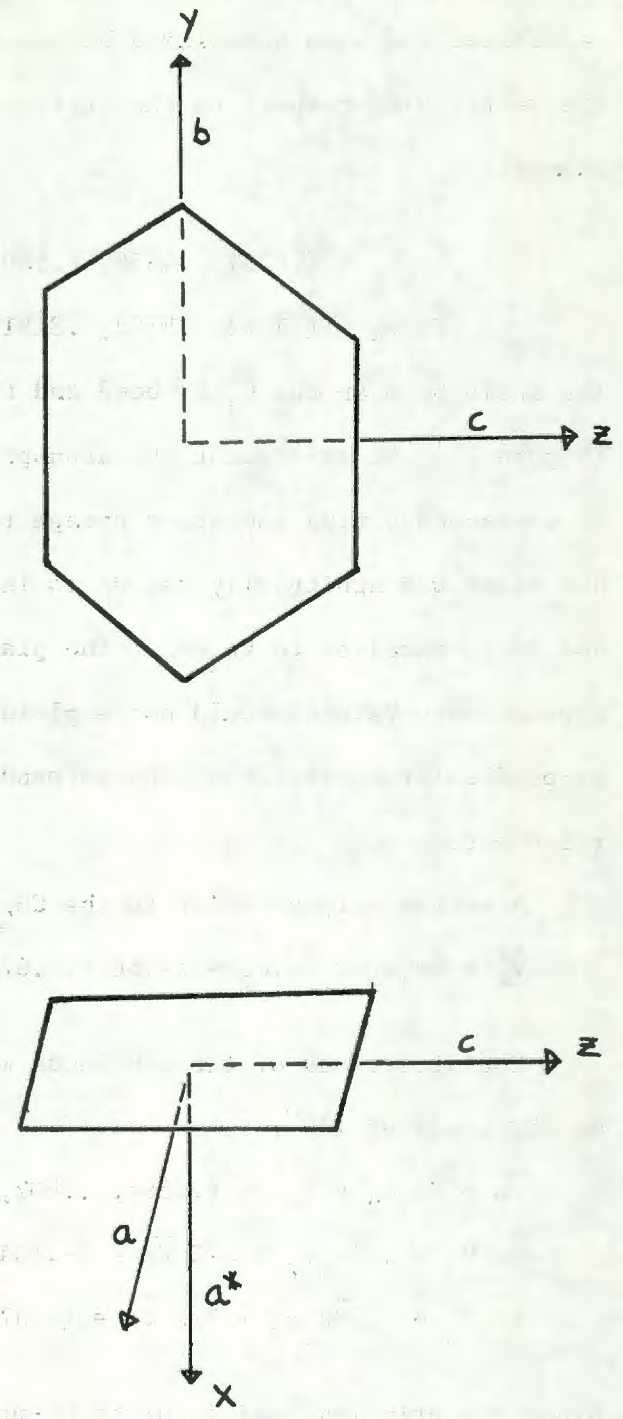

Figure 1. The orthogonal crystal axis system (xyz or a*bc) and its relationship to the crystalline axis system (abc).

The vectors for the distances between these atoms were calculated and when normalized became direction cosines of the vector with respect to the crystal axis system. Thus for example:

$$\vec{V}c_1c_2 = (.6751, .4559, -.5800)$$
$$\vec{V}o_1o_2 = (.2062, .5352, .8191)$$

The angle between the C_1-C_2 bond and the CO_2 plane is 15° (Figure 2). At this point the assumption was made that $\vec{V}c_1c_2$ is unchanged during radiation damage to the crystal. Then the HCH plane was arbitrarily set up to include the C_1-C_2 bond and to be parallel to $\vec{V}o_1$-o_2. The planar configuration was chosen since Valenti could not explain his results using the perpendicular model (28). The perpendicular model was not ruled out.

A vector perpendicular to the CH_2 plane is

$$\vec{V}_\perp = \vec{V}o_1o_2 \times \vec{V}c_1c_2 = (-.6878, .6755, -.2685)$$

The directions of the C-H bonds were established assuming an HCH angle of 120°.

$$\vec{V}p = \vec{V}c_1c_2 \times \vec{V}_\perp = (.2694, .5802, .7696)$$
$$\vec{V}c_1H_1 = .5\vec{V}c_1c_2 + 3/2\ \vec{V}p = (-.1043, .2745, .9565)$$
$$\vec{V}c_1H_2 = -.5\vec{V}c_1c_2 - 3/2\ \vec{V}p = (-.5709, -.7305, -.3765)$$

Since the principal values of an α-proton coupling tensor change very little from one saturated hydrocarbon to another (if delocalization of the odd electron is not critical), those values measured in the malonic acid radical, $\cdot CH(COOH)_2$, were used.

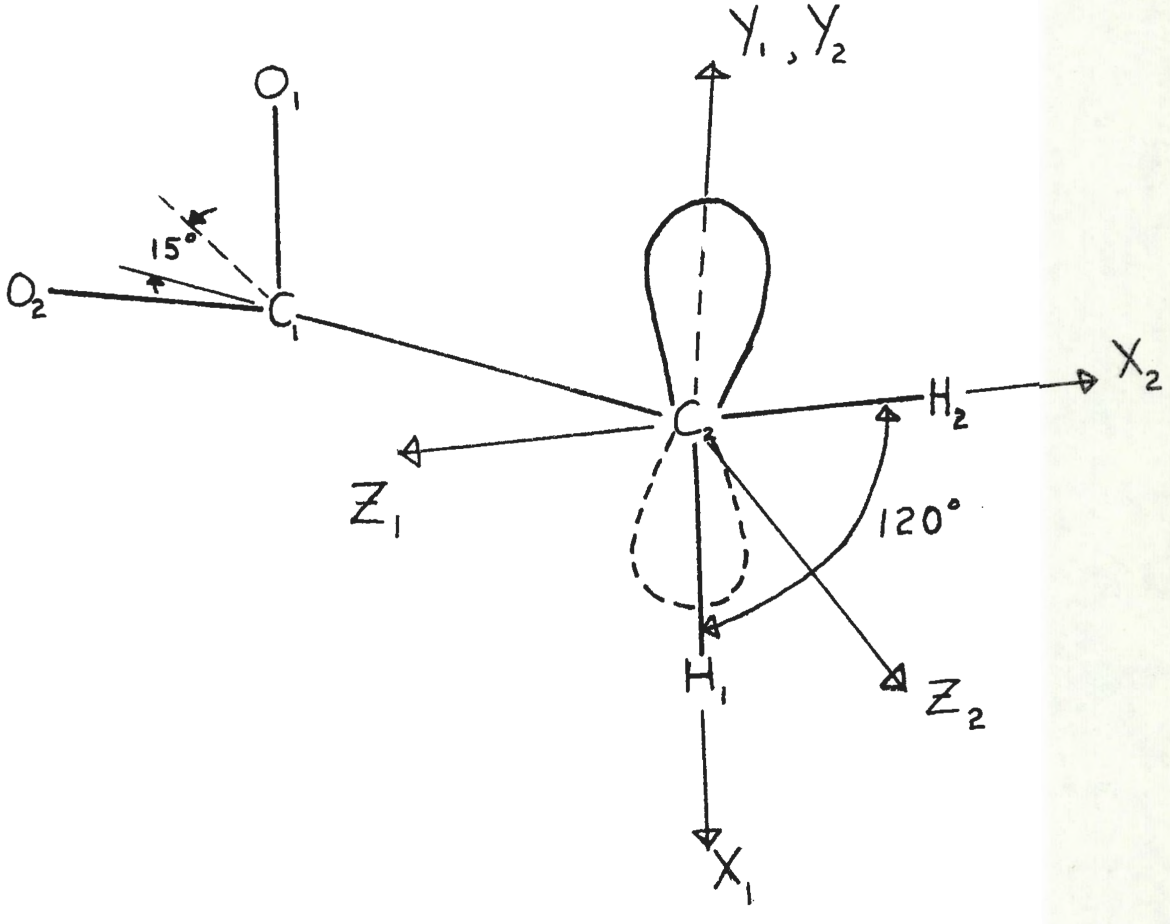

Figure 2. Locations of the hyperfine axes in the $\cdot CH_2CO_2^-$ radical(planar configuration).

$A = -29.$

$B = -61.$

$C = -91.$

Figure 2 shows the $CH_2CO_2^-$ radical and the assumed orientation of the molecule with the principal axes assigned as shown. The principal values A, B, C, were designated to be along the C-H bond, the p_z orbital axis, and in the CH_2 plane, perpendicular to the C-H bonds. These directions correspond to vectors $\vec{u}$, $\vec{v}$, and $\vec{w}$ in the crystal axis system. Thus the direction cosines for the A tensor were calculated to be

		x	y	z
H_1	u_1	-.1043	.2745	.9565
	v_1	-.6878	.6755	-.2685
	w_1	.7194	.6849	-.1175
H_2	u_2	-.5709	-.7305	-.3765
	v_2	-.6878	.6755	-.2685
	w_2	.4500	.1047	-.8871

3. Experimental

3.1 Growing of crystals

Various methods were used to grow the crystals needed for use in the spectrometer. All of the methods depended on the slow evaporation of water from saturated aqueous solutions. A 2.5:1 mass ratio of the zinc acetate to water worked best. A 115 ml solution in a 600 ml beaker resulted in well formed crystals but required from 2-7 days. If watch glasses are used, crystals can be grown overnight easily. Usually the above procedures are successful only on the first cycle because of the contamination of the solution on standing.

Another proven method was adding ZnO to 3-3.5 g concentrated acetic acid in 80-100 ml H_2O until a neutral solution resulted (no excess ZnO should be added). The solution was allowed to stand in a 150 ml beaker for 48-72 hours with the "hood" sliding window 1 inch above the beaker. Perfect crystals were produced every time this method was tried.

Acetic anhydride and ZnO were used together with D_2O to obtain the crystals for study of the effect on the satellite lines observed in the spectra. The crystals $(Zn\ (CH_3CO_2)_2 \cdot 2D_2O)$ were grown by slow evaporation of the solution from watch glasses.

3.2 Identification of Crystal Axes

3.2.1 X-Ray Diffraction

The outward appearance of the monoclinic crystals of zinc acetate dihydrate showed clearly which axis was the b axis, the two-fold axis. But to insure that this identification was correct an x-ray diffraction pattern was taken on an oscillation photograph. The crystal was glued to a glass fiber so that the incident x-ray beam was perpendicular to the assumed b axis. The crystal was rotated about the b axis and a photograph was taken. From the distances between the layer lines in the photograph the repeat distance of the Bravais lattice along the direction of the b axis was obtained. By a simple calculation using Braggs Law the length of the unit cell along the b axis was found to be 5.18A^{o}, which compared favorably with the value (5.32A^{o}) found by van Niekirk, et. al., for the unit cell dimension along the b axis (18).

3.2.2 Crystal Alignment

The orientation of the crystal in the spectrometer cavity was critical in order to determine the precise location of the magnetic field with respect to the crystal axis system. Two angles of rotation were needed to completely describe the 3-dimensional system. The crystal was rotated about one angle in the cavity but the other angle was varied outside the cavity. A Baush and Lomb microscope was set up with a revolving platform as a work pedestal. The turntable was calibrated such that 1 revolution = 360 units or degrees. The crystal was mounted on a quartz rod (28) with the (100) face parallel to the axis of the rod. The rod was clamped to the pedestal so that the crystal was centered on the turntable and the rod itself was positioned perpendicular to a tangent on the periphery of the turntable. The crystal was oriented on the rod by locating the b axis with respect to the axis of the rod with the aid of an eyepiece with crosshairs. The axis of the rod was positioned parallel to one of the crosshairs. The turntable was rotated the desired amount in degrees and the edges of the crystal parallel to the b axis were lined up with the reference crosshair.

3.3 Radiation Dosage

The single crystals were exposed to x-irradiation at 50KV and 20 ma from 2-4 hours using a molybdenum target. The crystals were placed on scotch tape and mounted in the open windows of the x-ray machine allowing the port covers to be closed at all times. The irradiations were made at room temperature.

3.4 ESR Spectrometer

The ESR spectrometer used was a Varian V-4502-13 with a Fieldial V-Fr 2503 magnetic field regulation and a nine inch magnet, using 100 KC modulation, and a conventional reflection type cavity equipped with a Varian variable temperature control unit.

The quartz rods on which the crystals were mounted had two flats ground parallel to each other on both ends of the rod. The end opposite the mounted crystal was clipped to an angle indicator positioned over the center of the spectrometer cavity. It was estimated that the angular position of the crystal could be measured accurately within $\pm 1^{\circ}$ with this apparatus (28).

The crystal was positioned in the yz plane by use of the microscope. The angle of rotation was designated as (ϕ) and the angle of rotation corresponding to the angle indicator above was called (θ) (Figure 3). All spectra taken were labeled by ($\frac{\theta}{\phi}$) for easy identification. The crystal was mounted with

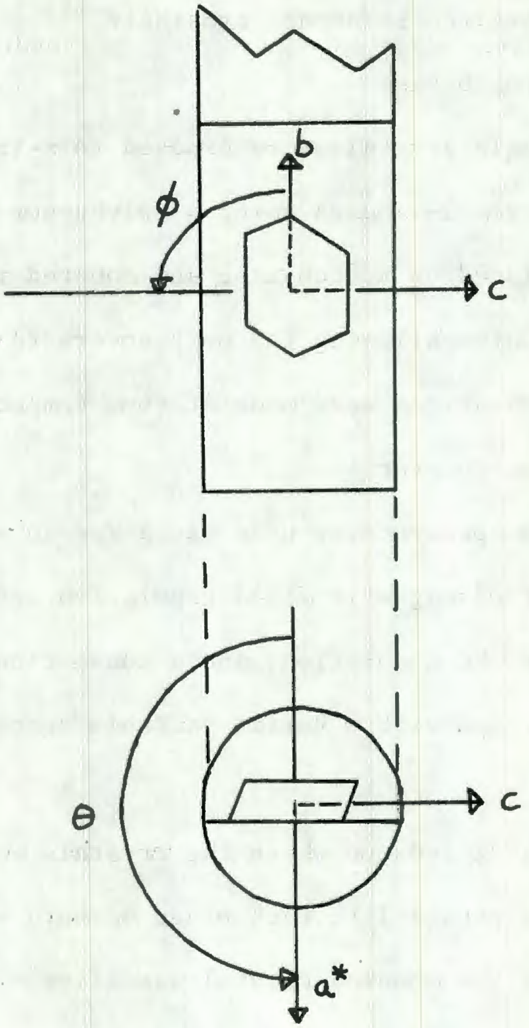

Figure 3. Single crystal of $Zn(CH_3CO_2)_2 \cdot 2H_2O$ mounted on a quartz rod with the b axis coincident with the axis of the rod. Crystal rotated by ϕ and rod rotated by θ.

its x axis extending into the rod and perpendicular to the axis of the rod. A complete data run was made by starting with the magnetic field along the -x axis((0°) direction) and incrementing by 15° until the field was along the +x axis - this was done for $\phi = 0, 15, 30, 45, 60, 75, 90$ degrees. Each spectrum was displayed on an x-y plotter and the magnetic field reading for each line was taken from a gauss field dial on the spectrometer.

3.5 Synthesis of Zn $(CH_2DCO_2)_2 \cdot 2H_2O$

Ethylene oxide $\left(\underset{O}{CH_2-CH_2}\right)$ was chosen as one of the starting materials because its ring is easily opened by a suitable reducing agent (7). $LiAlD_4$ was chosen as the reducing agent and the following reaction was carried out in a 500 ml, 3-necked flask immersed in an ice bath;

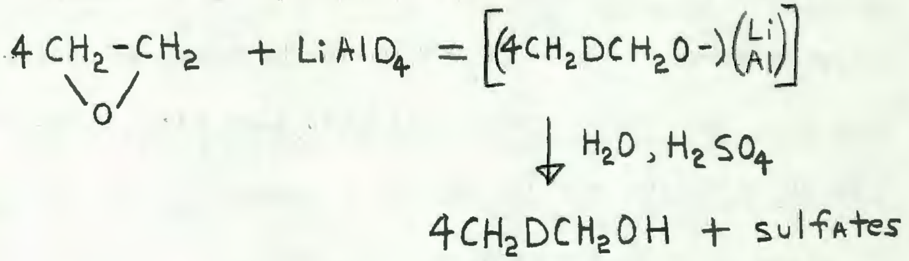

$$4\,\underset{O}{CH_2-CH_2} + LiAlD_4 = \left[(4CH_2DCH_2O-)\binom{Li}{Al}\right] \xrightarrow{H_2O,\ H_2SO_4} 4CH_2DCH_2OH + \text{sulfates}$$

The solvent used was triglyme [1, 2-Bis (2-methoxyethoxy) ethane] since its boiling point (220-225°C) was well above that of water and CH_2DCH_2OH. The solvent was purified by first using KOH pellets and letting solution stand for 72 hours. Approximately 250 ml was poured into a distillation flask and 6 g $LiAlH_4$ was added. After the initial reaction of the H_2O and $LiAlH_4$ had subsided, the solution was distilled under vacuum to obtain the high boiling triglyme. The operating pressure was .43 mm Hg. The distilling temperature was 61-62°C. 50 ml of the solvent was then placed in the 3-necked flask, with 3 g of $LiAlD_4$. The ethylene oxide was added to 50 ml of chilled triglyme in a 250 ml round bottomed flask on a "top loader" balance so that the ethylene oxide could be added by weight. 12.5 g of ethylene oxide was added to the triglyme and the solution was poured into a dropping funnel on the reaction vessel. The solution was allowed to run into the flask slowly. A condenser was placed on the reaction vessel with a 0°C water flow in order to minimize the loss of ethylene oxide (b.p.10°C). After the reaction appeared complete, 58 ml of 3M H_2SO_4 was added and the increase in viscosity that resulted indicated that the sulfates were coming out of solution. The CH_2DCH_2OH and water were distilled over at a temperature range of 78 to 102°. Yields were calculated to be around 96% giving approximately 13 g of CH_2DCH_2OH in the water alcohol mixture.

The deuterated alcohol was then added slowly by burette to an oxidizing mixture of

40.7 ml H_2SO_4
56.2 g $K_2Cr_2O_7$
212.0 ml H_2O

in a 3-necked flask immersed in an ice bath. The following reaction took place while keeping the solution in the vicinity of 25°C.

$$3CH_2DCH_2OH + 2K_2Cr_2O_7 + 8H_2SO_4 = 3CH_2DCOOH + 2K_2SO_4 + 2Cr_2(SO_4)_3 + 11H_2O \quad (10)$$

The solution was refluxed for 5-10 minutes and then the CH_2DCOOH and water were distilled over at 100°C. Yields ranged from 65 to 75% giving 10-12 g of the acid.

ZnO was added to 85 ml of the acid solution (3-3.5gCH_2DCOOH) until the solution turned neutral but not cloudy (excess ZnO).

$$ZnO + 2CH_2DCOOH = Zn(CH_2DCO_2)_2 + H_2O$$

The slow evaporation of the product solution from a 150 ml beaker produced the needed crystals for ESR study.

Vapor-phase chromatography was used to identify the alcohol and acetic acid in their product solutions and the peaks in comparison to those of a standard were indicative of relative amounts present also. The VPC analysis did not contain any impurity peaks.

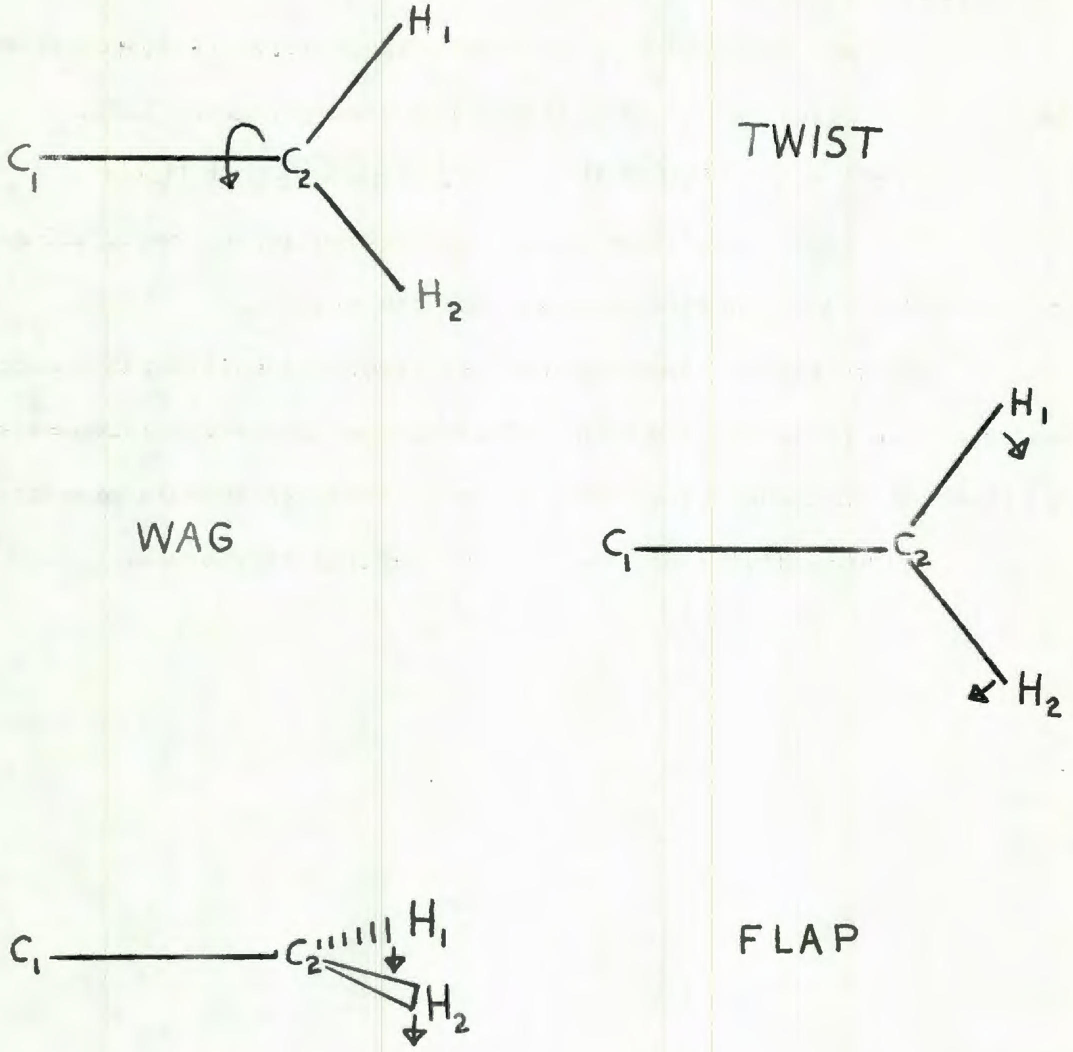

Figure 4. Bending vibrations of the CH_2 group in the $\cdot CH_2CO_2^-$ radical.

4. Problem Solution and Spectral Analysis

4.1 Characterization of the $\cdot CH_2CO_2^-$ radical

4.1.1 Theoretical Formulation

The main computer program developed in this investigation was constructed around two main subprograms; (a) a method for prediction of the transition frequencies and intensities (PREDICT); and (b) a least squares method for obtaining the best fit between calculated and observed frequencies. This main program shall be hereafter referred to as OPTIM. The method for prediction of transition frequencies and intensities was available in PREDICT and the input to this program required a precise orientation of the CH_2 group. A change in this orientation produced a change in the predicted transition frequencies and intensities because of a simultaneous change in the direction cosines. Thus a means of describing the location of the CH_2 group was needed in order to perform any repetitive calculation such as a least squares fit. The use of a least squares fit required that certain parameters be chosen and the angles concerned with the location of the CH_2group were considered good choices. The selection of parameters was based on the criteria of at least determining whether the CH_2 group was planar or perpendicular to the rest of the molecule. The twist of the CH_2 group was then chosen as the first parameter which involved a rotation about the C-C bond. (Figure 4) Three more parameters were chosen to account for the wag, flap, and HCH angle of the CH_2 group. The relationship of these three parameters to the direction cosines of the CH_2 principal axes were solved by using a similarity transformation technique. Any random vector (a, b, c) can be rotated to a position along the z axis by the following transformation

$$\begin{pmatrix} \frac{b}{d} & -\frac{a}{d} & 0 \\ \frac{ac}{d} & \frac{bc}{d} & -d \\ a & b & c \end{pmatrix} \begin{pmatrix} a \\ b \\ c \end{pmatrix} = \begin{pmatrix} 0 \\ 0 \\ 1 \end{pmatrix}$$

where $d = (1-c^2)^{\frac{1}{2}}$ and $a^2 + b^2 + c^2 = 1$.

The following matrix multiplications illustrate the formation of a transformation matrix which will rotate any other vector a number of degrees θ about the vector (a, b, c).

$$\begin{pmatrix} \frac{b}{d} & \frac{ac}{d} & a \\ -\frac{a}{d} & \frac{bc}{d} & b \\ 0 & -d & c \end{pmatrix} \begin{pmatrix} \cos\theta & \sin\theta & 0 \\ -\sin\theta & \cos\theta & 0 \\ 0 & 0 & 1 \end{pmatrix} \begin{pmatrix} \frac{b}{d} & -\frac{a}{d} & 0 \\ \frac{ac}{d} & \frac{bc}{d} & -d \\ a & b & c \end{pmatrix}$$

This transformation was permitted to operate on the direction cosines of the g and A tensors for each value of twist, wag, and flap. The direction cosines were updated each time a new set of parameters was calculated. The HCH angle was not involved in a rotation but was used to set up the planar configuration for each new set of parameters. This configuration was assumed because initial calculations using PREDICT showed the planar form to yield the more correct "stick spectrum".

PREDICT was modified to include the calculation of an effective g value which was necessary due to the 2 magnetically inequivalent sites of $Zn(CH_3CO_2)_2 \cdot 2H_2O$ for orientations of the magnetic field in other than the xz plane. The transitional frequencies computed by PREDICT for each site were shifted upfield or downfield depending on the effective g value. The calculation of an effective g value was made in section 1.2. The principal values of the g tensor used as initial parameters in this investigation were 2.0020, 2.0042, and 2.0034, which were values corresponding to directions perpendicular to the CH_2 group, parallel to the C-C bond, and in the plane of the CH_2 group perpendicular to the C-C bond. Due to their importance these variables were also selected as possible parameters along with the 6 principal values of the 2 coupling tensors. Both coupling tensors were included because other work has shown that hyperfine coupling with α-protons is highly anisotropic (16), but the principal values are expected to be similar (3).

The transitional frequencies computed by PREDICT were placed in a matrix to be used to calculate differences between selected frequencies. These differences were then compared with observed differences taken from the experimental spectra and the results formed a reference matrix to be used in the least squares fit, which was developed for use with linear or non linear equations. In this investigation a highly non linear situation was assumed to exist and the derivative matrix was formed by varying each parameter only a small amount. The mathematical formulation of the least squares method is as follows:

ϵ_i = error between calculated and observed value -ith point

y_i = ith calculated point

y_i^o = ith point, observed value

a_j = jth independent parameter

$d_{ij} = \partial y_i / \partial a_j$

$\epsilon_i = y_i - y_i^o$

$$\Delta y_i = \sum_j \left(\frac{\partial y_i}{\partial \Delta a_j}\right) a_j = \sum_j d_{ij} \Delta a_j$$

The least squares restriction: $\frac{\partial}{\partial \Delta a_k} \sum_i (\epsilon_i + \Delta y_i)^2 = 0$

$$\frac{\partial}{\partial \Delta a_k} \sum_i \left(\epsilon_i + \sum_j d_{ij} \Delta a_j\right)^2 = 2 \sum_i \left(\epsilon_i + \sum_j d_{ij} \Delta a_j\right) d_{ik} = 0$$

$$\sum_i d'_{ki} \epsilon_i + \sum_{i,j} d_{ij} d_{ik} \Delta a_j = 0$$

$$\sum_i d'_{ki} \epsilon_i + \sum_{i,j} d'_{ki} d_{ij} \Delta a_j = 0$$

Define D = matrix of elements d_{ij}

E = column matrix of elements ϵ_i

Δx = column matrix of elements Δa_j

$D'E + D'D\Delta x = 0$

Thus $\Delta x = -(D'D)^{-1}D'E$

The matrix Δx represents the best change in each independent parameter for the best fit of the data.

The elements of this matrix were added to the corresponding original parameters and the entire program of OPTIM was repeated until successive iterations produced only very small changes in the parameters. The derivative matrix (d_{ij}) was generated by introducing incremental changes in each parameter while holding others constant and calculating the resulting effect on the differences between the transition frequencies.

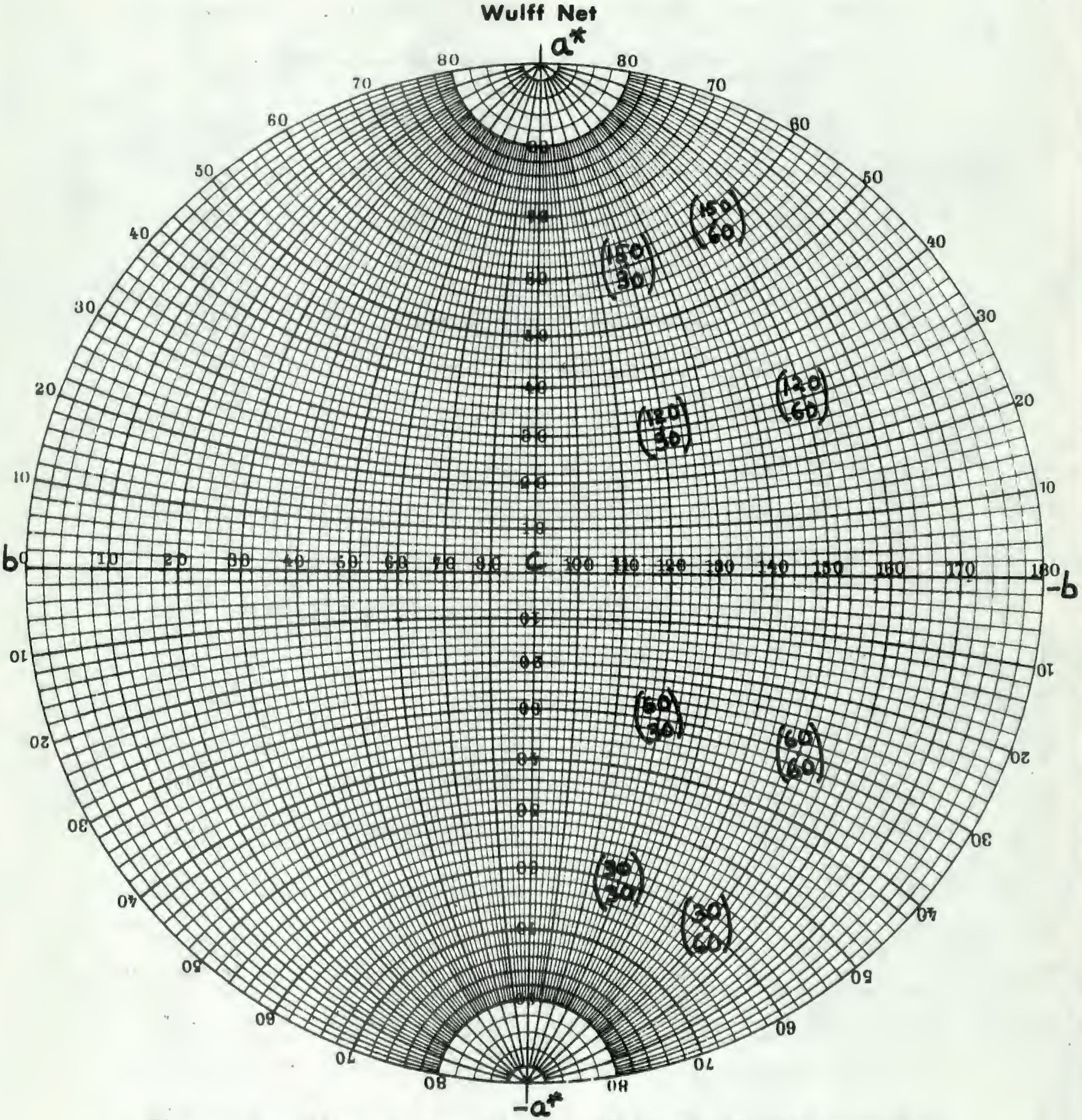

Figure 5. Stereographic net used to catalogue magnetic field orientations.

A measure of the uncertainty in each parameter can be calculated using a probabalistic approach. From the least squares analysis the best changes in each parameter for the best fit were

$$\Delta x = (D'D)^{-1} D'E$$

If there were no error involved

$$E = D\Delta x$$

where E = calc -obs points

but, in general, $E = D\Delta x + e$

Uncertainty in $\Delta x = \langle \Delta x \rangle$

"True" value of $\Delta x = \Delta x$

Value of Δx at some time is $\hat{\Delta x}$

$$\begin{aligned}
\langle \Delta x \rangle^2 &= \text{Average of } (\hat{\Delta x} - \Delta x)(\Delta x - \Delta x)' \\
&= \text{Average of } \left[(D'D)^{-1} D'E - \Delta x\right]\left[(D'D)^{-1} D'E - \Delta x\right]' \\
&= (D'D)^{-1} D' \,(\text{Avg of } ee')\, D(D'D)^{-1} \\
&= \sigma^2 (D'D)^{-1}
\end{aligned}$$

where σ^2 is the standard deviation squared (avg of ee'). This expression shows that if D'D is diagonal then the errors are truly determined.

4.1.2 Data Obtained

With the crystal mounted as described in section 3.4, ESR spectra were taken at 15° increments of θ and Ø. For a corresponding value of θ, Ø was varied from 0° to 180° and the resulting number of possible magnetic field orientations was 79. The number of spectra was so extensive that a stereographic net was used to catalogue the different orientations $(\frac{\theta}{\emptyset})$. A typical Wulff net is shown in Figure 5 with the crystal axis system labeled and some of the field orientations indicated.

TABLE I. Data used for the least squares fit.

Field Orientation	Field Dial Reading*	Differences Taken	Field Orientation	Field Dial Reading*	Differences Taken
$\begin{pmatrix}90\\0\end{pmatrix}$	20.50s	29.78	$\begin{pmatrix}180\\0\end{pmatrix}$	17.84s	20.96
	30.84s	10.34		38.80s	26.61
	50.28s			44.45s	
	60.61s			65.38s	
$\begin{pmatrix}120\\0\end{pmatrix}$	22.55s	23.50	$\begin{pmatrix}90\\90\end{pmatrix}$	14.19s	18,50
	27.20w	17.17		19.70w	28.62
	35.10w			37.24s	
	46.05s			38.30w	
	50.60w			43.40s	
	58.50w			48.30w	
	63.20s			56.95w	
				61.84s	
$\begin{pmatrix}135\\0\end{pmatrix}$	22.20s	40.58			
	27.45w		$\begin{pmatrix}15\\90\end{pmatrix}$	13.50s	19.39
	36.80w			17.40s	15.49
	42.49s			27.80w	29.21
	48.12w			32.89s	
	57.20w			37.88s(2)	
	62.78s			42.81s	
				62.00s(2)	
$\begin{pmatrix}150\\0\end{pmatrix}$	21.60s	17.70			
	26.01w	24.09	$\begin{pmatrix}30\\90\end{pmatrix}$	12.54s	18.31
	34.29w			17.98s	31.75
	39.30s			25.78w	12.87
	45.69s			30.85s	26.31
	50.23w			39.49s(2)	
	48.68w			44.29s	
	63.29s			49.26w	
				62.10s(2)	
$\begin{pmatrix}165\\0\end{pmatrix}$	20.16s	18.12			
	24.95w	26.07	$\begin{pmatrix}45\\90\end{pmatrix}$	12.08s	17.58
	33.19w			18.43s	32.69
	38.28s			24.84w	11.23
	46.23s			29.66s	26.34
	51.02w			34.71w	
	59.38w			39.61s(2)	
	64.22s			44.77s	
				49.54w	
				61.83s(2)	

*Gauss field dial on spectrometer.
Readings taken from a 100 gauss sweep.
s, strong; w, weak; ( ), no. of lines overlapping.

Field Orientation	Field Dial Reading*	Differences Taken
$\begin{pmatrix}60\\90\end{pmatrix}$	11.90s	17.42
	17.40s	32.71
	28.32s	11.92
	38.90s(2)	27.21
	44.61s	
	61.25s(2)	
$\begin{pmatrix}75\\90\end{pmatrix}$	12.40s	17.80
	16.09s	19.37
	24.46w	14.11
	30.02s	
	35.46s	
	41.09s	
	56.03w	
	61.00s(2)	
$\begin{pmatrix}45\\15\end{pmatrix}$	22.80s	4.15
	26.95s	
	46.20s(2)	
	54.60s(2)	
	69.30w	
	75.65s(2)	
$\begin{pmatrix}60\\15\end{pmatrix}$	23.20s	53.00
	28.00s	44.45
	43.68s(2)	48.20
	50.63w	
	56.00s(2)	
	72.45s	
	76.20s	
$\begin{pmatrix}75\\15\end{pmatrix}$	25.10s	49.98
	30.11s	40.42
	42.25s(2)	45.43
	57.99s(2)	44.97
	70.53s	
	75.08s	
$\begin{pmatrix}105\\15\end{pmatrix}$	30.11s(2)	15.20
	43.27s	
	47.04w	
	58.47s	
	71.73s(2)	

Field Orientation	Field Dial Reading*	Differences Taken
$\begin{pmatrix}120\\15\end{pmatrix}$	30.85s(2)	10.02
	46.40s	
	51.25s(2)	
	56.42s	
	72.00s(2)	
$\begin{pmatrix}150\\15\end{pmatrix}$	26.19w	41.61
	31.39s(2)	
	47.08s	
	51.40s	
	56.30s	
	68.66w	
	73.00s(2)	
$\begin{pmatrix}165\\15\end{pmatrix}$	25.51w	43.75
	30.20s(2)	
	48.63s(2)	
	56.30s(2)	
	69.00w	
	73.95s(2)	
$\begin{pmatrix}45\\30\end{pmatrix}$	21.70s	55.93
	28.18s	51.90
	47.03s(2)	49.45
	51.35s	
	55.25s	
	68.60w	
	73.60s	
	77.63s	
$\begin{pmatrix}60\\30\end{pmatrix}$	21.58s	55.56
	29.63s	42.62
	45.26s(2)	50.67
	53.40s	47.51
	56.78s	
	72.25s	
	77.14s	
$\begin{pmatrix}75\\30\end{pmatrix}$	23.37s	53.38
	30.56s	40.84
	44.63s(2)	48.03
	55.78s(2)	
	71.40s	
	76.75s	

Field Orientation	Field Dial Reading*	Differences Taken
$\begin{pmatrix}105\\30\end{pmatrix}$	16.30s	12.15
	19.80s	
	33.25s	
	39.25s(2)	
	45.40s	
	58.80s	
	62.30s	
$\begin{pmatrix}150\\30\end{pmatrix}$	12.90w	12.08
	18.60s(2)	0.00
	33.32s	
	39.52s(2)	
	45.40s	
	60.40s(2)	
$\begin{pmatrix}45\\45\end{pmatrix}$	21.40s	56.79
	29.80s	25.05
	49.25s(3)	43.80
	54.85s	33.45
	73.60s	52.20
	78.19s	43.39
		23.34
$\begin{pmatrix}60\\45\end{pmatrix}$	21.32s	57.28
	30.95s	24.80
	47.84s(3)	41.95
	55.75s	34.41
	72.90s	9.63
	78.60s	51.58
		47.65
		22.87
$\begin{pmatrix}75\\45\end{pmatrix}$	22.76s	55.54
	31.60s	41.10
	48.30s	46.90
	53.92s(2)	8.64
	72.70s	49.74
	78.50s	
$\begin{pmatrix}105\\45\end{pmatrix}$	17.90s	48.27
	32.90w	27.70
	38.38s(2)	
	45.60s(2)	
	61.10s	
	66.17s	
$\begin{pmatrix}130\\45\end{pmatrix}$	21.00s(2)	25.50
	34.60s	26.00
	39.40s	30.30
	46.48s(2)	
	60.60s	
	64.90s	
$\begin{pmatrix}135\\45\end{pmatrix}$	14.80w	16.35
	21.78s(2)	30.30
	33.45s	
	40.97s	
	44.90s	
	49.80s	
	60.13s	
	63.75s	
$\begin{pmatrix}150\\45\end{pmatrix}$	13.13w	14.57
	19.50s(2)	
	32.86s	
	41.19s(2)	
	47.43s	
	61.87s(2)	
	67.30w	
$\begin{pmatrix}15\\60\end{pmatrix}$	26.05s	21.50
	29.36s	
	48.05s	
	53.10s	
	76.30s(2)	
$\begin{pmatrix}30\\60\end{pmatrix}$	23.50s	23.27
	30.51s	16.91
	47.42s	7.01
	53.58s(3)	
	74.93s	
	78.00	
$\begin{pmatrix}45\\60\end{pmatrix}$	22.10s	25.68
	31.37s	56.45
	47.78s	42.58
	52.82s(3)	47.18
	73.95s	51.85
	78.55s	9.27

Field Orientation	Field Dial Reading*	Differences Taken
$\begin{pmatrix}60\\60\end{pmatrix}$	21.60s	25.85
	31.42s	56.35
	48.54s	41.85
	52.05s(3)	46.98
	73.08s	51.48
	78.40s	9.82
$\begin{pmatrix}75\\60\end{pmatrix}$	22.15s	55.10
	31.10s	41.32
	49.85s(3)	46.56
	72.08s	49.63
	77.56s	8.85
$\begin{pmatrix}105\\60\end{pmatrix}$	17.40s	49.08
	21.85s	11.80
	33.65s	32.83
	41.80s(2)	
	49.30s	
	61.00s	
	66.48s	
$\begin{pmatrix}120\\60\end{pmatrix}$	20.90s(2)	19.38
	31.62s	29.48
	42.05s(2)	34.04
	51.00s	14.66
	61.10s	
	65.66s	
$\begin{pmatrix}135\\60\end{pmatrix}$	19.85s(2)	19.70
	30.10s	
	41.47s(2)	
	49.80s	
	62.35s	
	68.50w	
$\begin{pmatrix}150\\60\end{pmatrix}$	18.32s	15.63
	21.30s	
	32.60s	
	42.30s(2)	
	48.23s	
	63.15s(2)	
$\begin{pmatrix}15\\75\end{pmatrix}$	25.80s	21.06
	29.80s	16.92
	41.10w	4.08
	46.72s	
	52.26s(2)	
	55.23s	
	75.80s(2)	
$\begin{pmatrix}30\\75\end{pmatrix}$	23.55s	21.83
	30.30s	14.70
	45.00s	6.75
	51.90s(2)	
	74.59s(2)	
$\begin{pmatrix}45\\75\end{pmatrix}$	21.95s	21.95
	30.70s	54.87
	43.90s	42.02
	51.82s(2)	13.20
	72.72s	8.75
	76.82s	50.77
		46.12
$\begin{pmatrix}60\\75\end{pmatrix}$	21.40s	22.81
	30.28s	55.25
	44.21s	41.90
	52.04s(3)	13.93
	67.45w	8.88
	72.18s	50.78
	76.65s	46.37
$\begin{pmatrix}75\\75\end{pmatrix}$	23.27s	53.48
	30.96s	42.16
	47.48s	46.39
	54.40s(2)	49.25
	59.50w	
	72.52s	
	76.75s	
$\begin{pmatrix}120\\75\end{pmatrix}$	19.00s(2)	19.75
	29.75s	34.15
	41.38s(2)	
	49.50s	
	63.90s	
$\begin{pmatrix}135\\75\end{pmatrix}$	10.10w	18.42
	18.90s	
	29.13s	
	40.67s(2)	
	47.55s	
	61.60s(2)	
$\begin{pmatrix}150\\75\end{pmatrix}$	11.10w	15.52
	16.28s	31.02
	20.40s	11.40
	31.80s	
	41.47s(2)	
	47.30s	
	62.75s(2)	
	67.95s	

Field Orientation	Field Dial Reading*	Differences Taken	Field Orientation	Field Dial Reading*	Differences Taken
$\begin{pmatrix}60\\15\end{pmatrix}$	27.48s	46.04			
	31.30s	38.65			
	42.20s(2)	42.22			
	58.75s(2)	42.47			
	69.95s				
	73.52s				
$\begin{pmatrix}90\\30\end{pmatrix}$	26.30s	49.90			
	31.20s	40.40			
	45.00s(2)	45.00			
	57.07s(2)	45.30			
	71.60s				
	76.20s				
$\begin{pmatrix}90\\45\end{pmatrix}$	25.20s	52.65			
	31.86s	40.64			
	47.60s(2)	45.99			
	53.90s(2)	47.30			
	72.50s				
	77.85s				
$\begin{pmatrix}90\\60\end{pmatrix}$	24.42s	52.48			
	30.88s	40.96			
	42.03w	46.02			
	46.52w	47.42			
	50.52s				
	55.67w				
	71.84s				
	76.90s				
$\begin{pmatrix}90\\75\end{pmatrix}$	25.67s	51.16			
	30.22s	42.59			
	45.55s	46.61			
	48.85s	47.14			
	53.87s				
	57.77s				
	72.81s				
	76.83s				

Each spectrum was analyzed with the aid of the "stick spectrum" predicted by PREDICT for a particular field orientation. The "stick spectrum" was plotted after arbitrarily assigning sites 1 and 2. The best lines were selected for taking differences; some spectra were not used because of too much overlap. Differences were taken within each site and between the 2 sites. These differences are tabulated in Table I for each spectrum that was usable in obtaining the least squares fit. The gauss field dial readings (from spectrometer) taken for each experimental spectrum are also tabulated. These readings correspond to the relative positions of resolvable lines in a 100 gauss sweep. The experimental spectra were taken at 133°K at a magnetic field of 3210 ± 50 gauss.

4.1.3 Correlation of data with Theory

The experimental spectra for selected field orientations are shown in Figures 7-9. The predicted spectra are plotted also to show the close fit that was obtained by least squaring the differences taken. Although 3 iterations were used, the most significant convergence of OPTIM occurred in the first iteration. The best fit was obtained using 166 differences selected from 55 different field orientations. More than one crystal is represented by these data and it was significant that two different irradiated crystals did not differ in their spectra and the differences obtained were within ± .5 gauss of each other. After 3 iterations of the least squares program the matrix containing the calculated minus

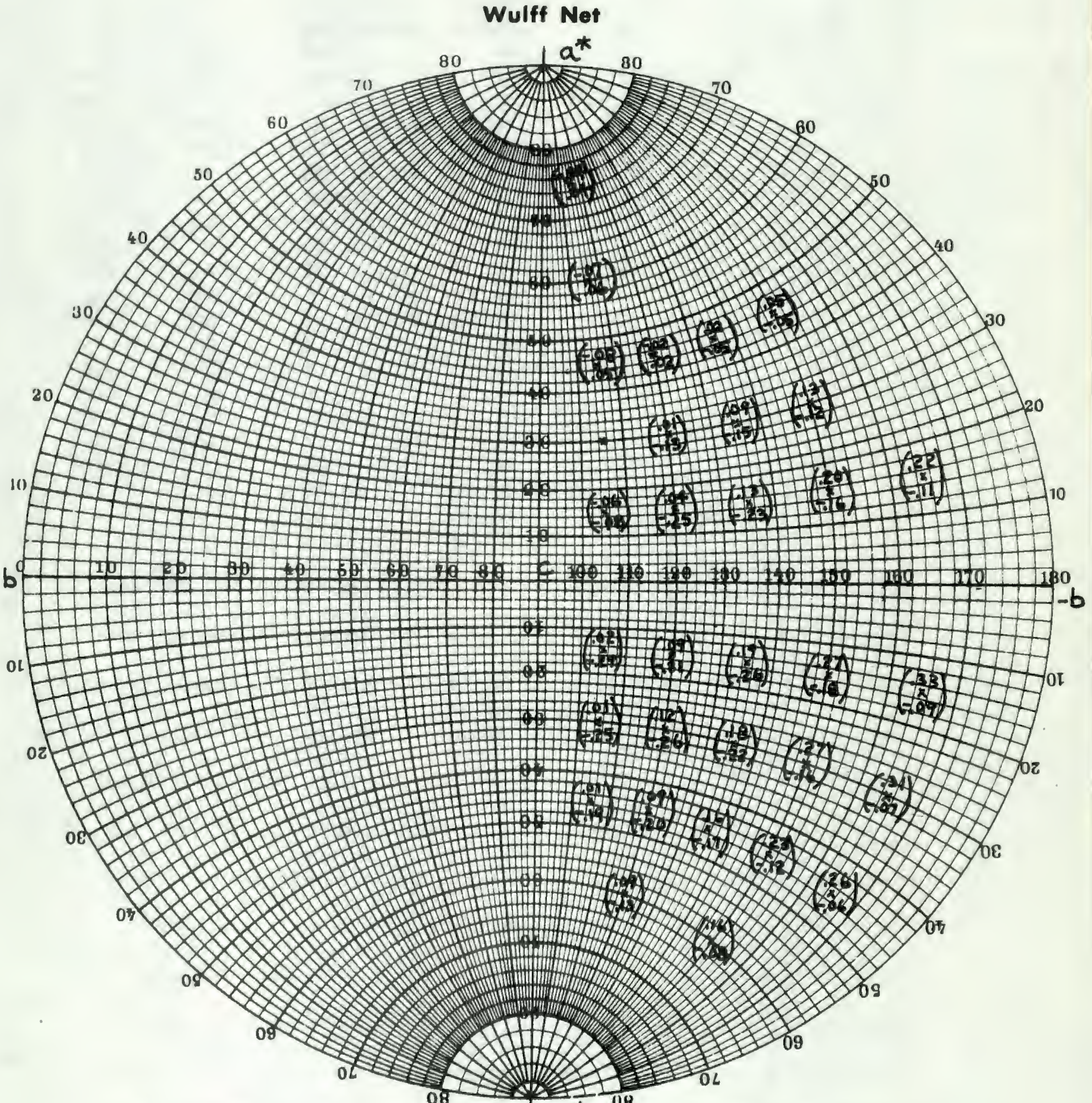

Figure 6. Errors in coupling constants for the methylene protons $\left(\frac{1}{2}\right)$ in $\cdot CH_2CO_2^-$ for a 1° error in angle ϕ.

observed differences was as follows: the error differences are read by rows and correspond to the same order as the observed differences in Table I.

.35	-.01	.26	-.48	.25	.12	-.21	-.10
-.09	-.28	.22	.30	.77	-.49	.28	.13
-.19	-.34	.11	.29	-.22	-.03	-.15	.08
-.22	.01	-.32	-.06	.26	-.37	-.45	.30
-.30	-.56	.57	.34	-.33	.23	-.35	-.32
.04	.27	.03	.39	-.09	.22	-.04	-.08
.26	.14	-.30	.04	.12	.28	.84	.31
.14	-.09	.45	.32	.22	-.00	-.14	.09
-.55	-.20	-.44	.09	-.11	-.00	.53	.20
-.37	-.03	.23	-.14	.25	.22	-.04	.61
-.02	-.11	.53	.30	.49	.38	-.14	-.13
-.47	.00	.11	.02	.10	-.01	.48	.56
-.26	.07	-.03	.04	.53	-.13	.35	-.03
-.13	-.04	.87	-.14	.28	.26	-.06	-.34
-.50	.26	-.21	.34	-.49	-.64	-.26	.00
-.33	-.64	.23	-.10	-.23	.00	-.41	-.78
-.88	.16	-.33	-.45	-.29	-.43	-.31	.38
.02	.05	-.68	-.44	-.11	.71	.46	.24
-.48	.82	.04	.31	.07	-.48	-.50	.10
-.10	-.36	-.09	-.36	.34	-.08	.38	-.12
-.36	.50	.07	.06				

The standard deviation for this data was calculated to be .335 gauss. The angle Ø involved in the rotation of the crystal in the spectrometer and defining the center of a transition were considered the main sources of error. An error analysis using the proton coupling constants is shown in Figure 6. The errors in the coupling constants for protons 1 and 2 for a 1° error in angle Ø are displayed on a Wulff net for selected orientations. In general, as the angle varies, the error in one coupling constant increases while the error in the other coupling constant decreases. An average error estimate for each coupling constant is ± .15 gauss. The coupling constants for field orientations close to the b and c axes are very sensitive to changes in Ø. But as the field vector approaches either the -a* or a*

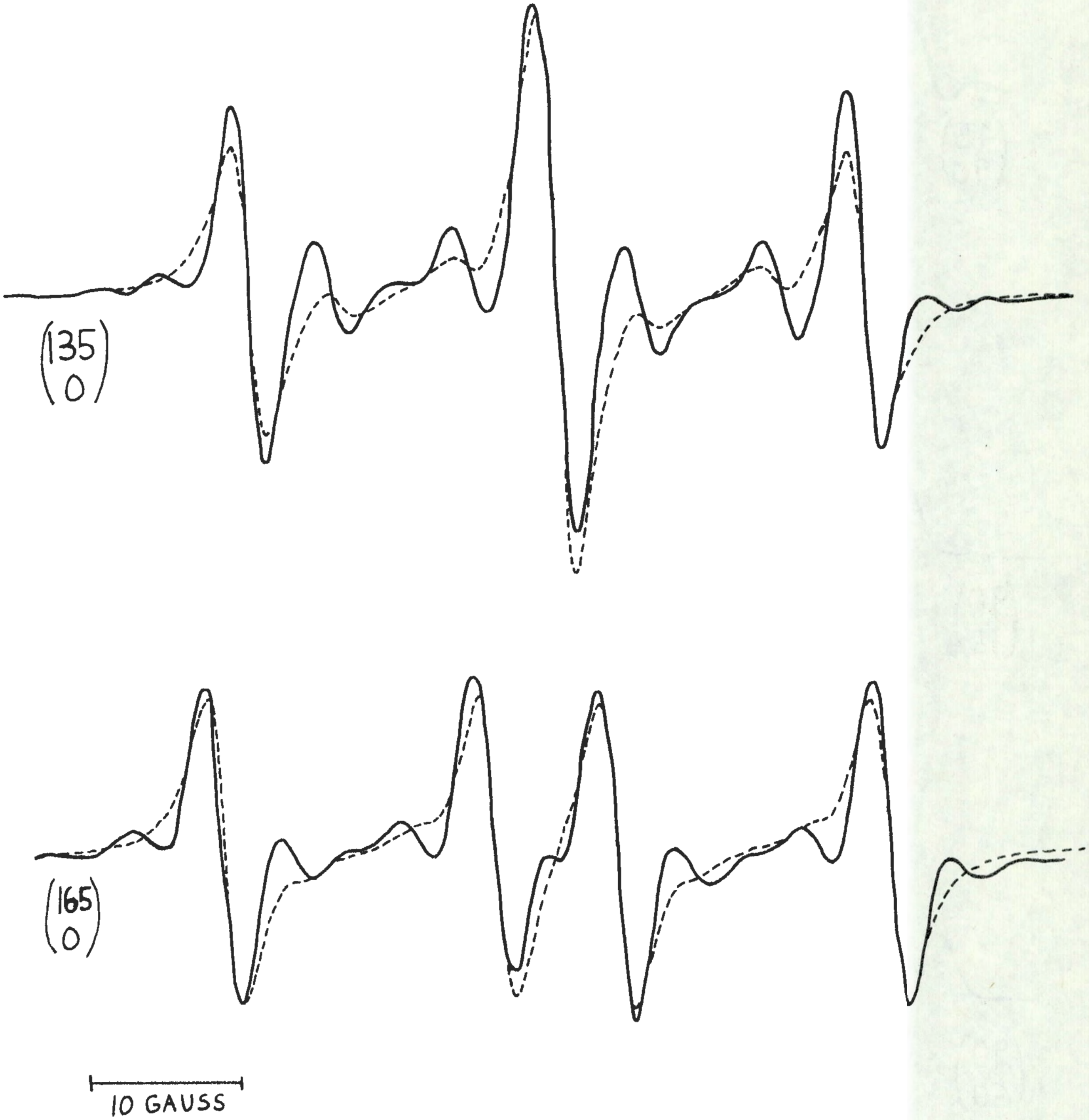

Figure 7. ESR spectra of the $\cdot CH_2CO_2^-$ radical at 133°K. Magnetic field perpendicular to two-fold axis.

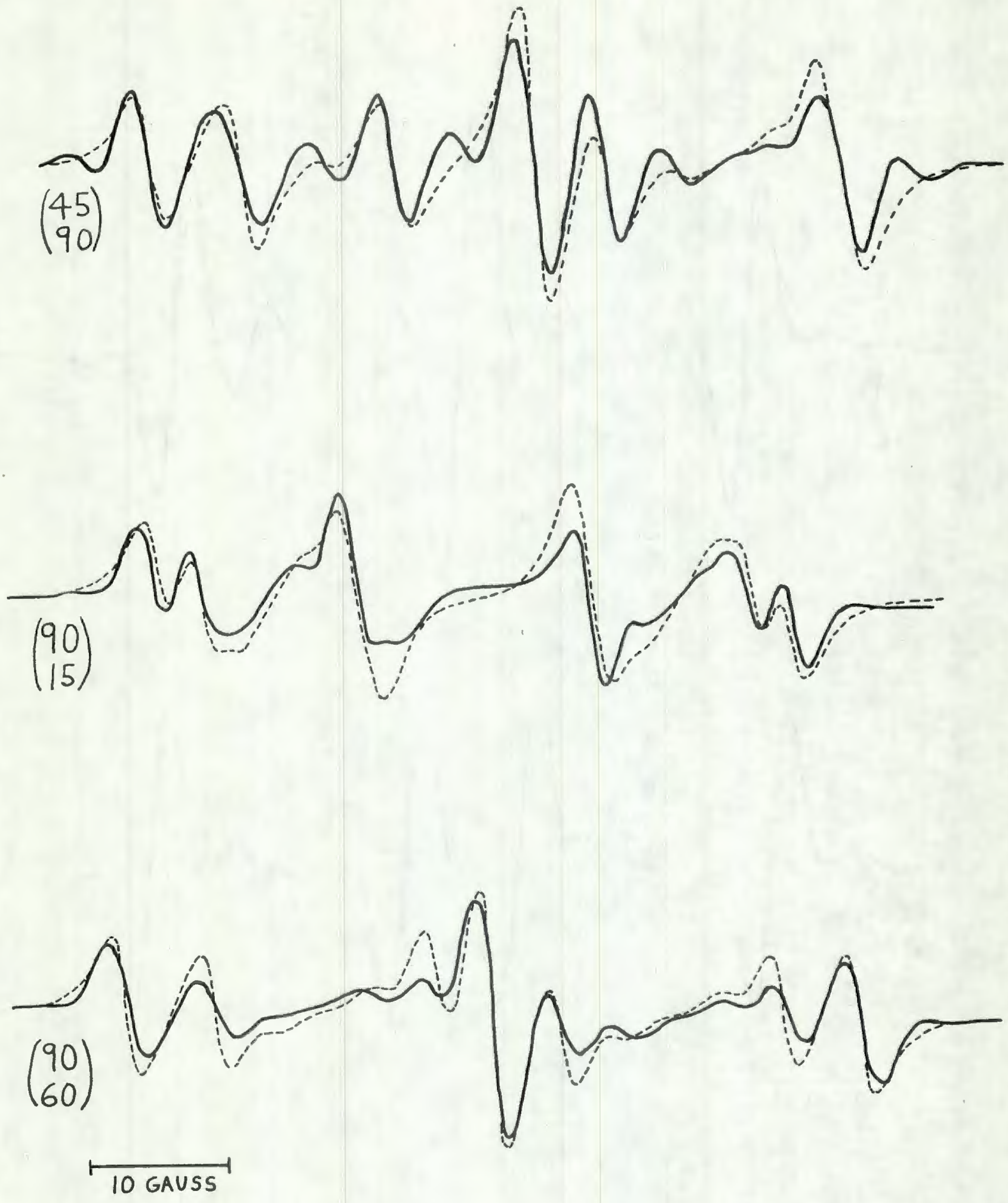

Figure 8. ESR spectra of the ·CH$_2$CO$_2^-$ radical at 133°K. Magnetic field perpendicular to z axis for $\binom{45}{90}$ spectrum and perpendicular to x axis for other spectra.

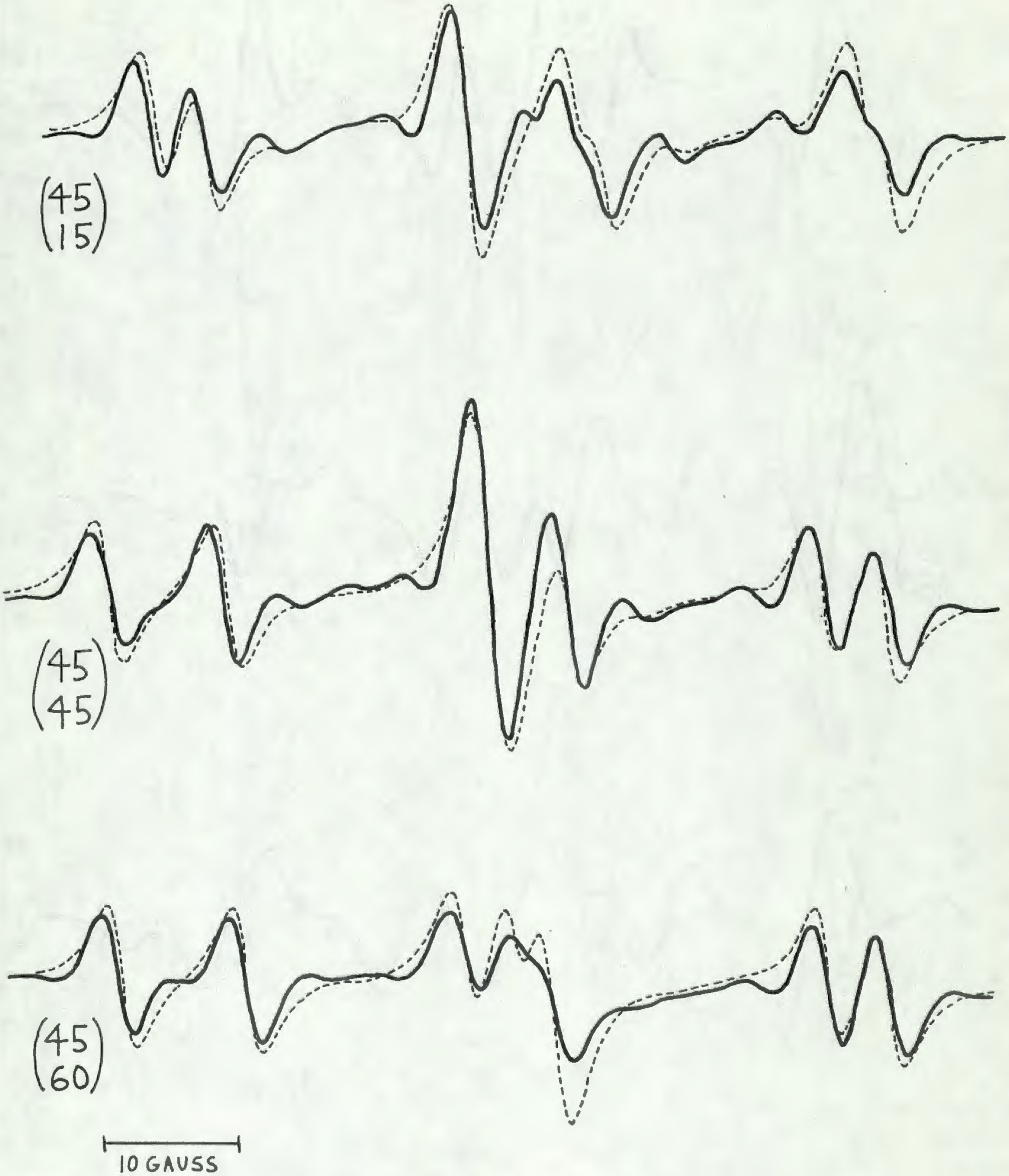

Figure 9. ESR spectra of the $\cdot CH_2CO_2^-$ radical at 133°K for selected magnetic field orientations.

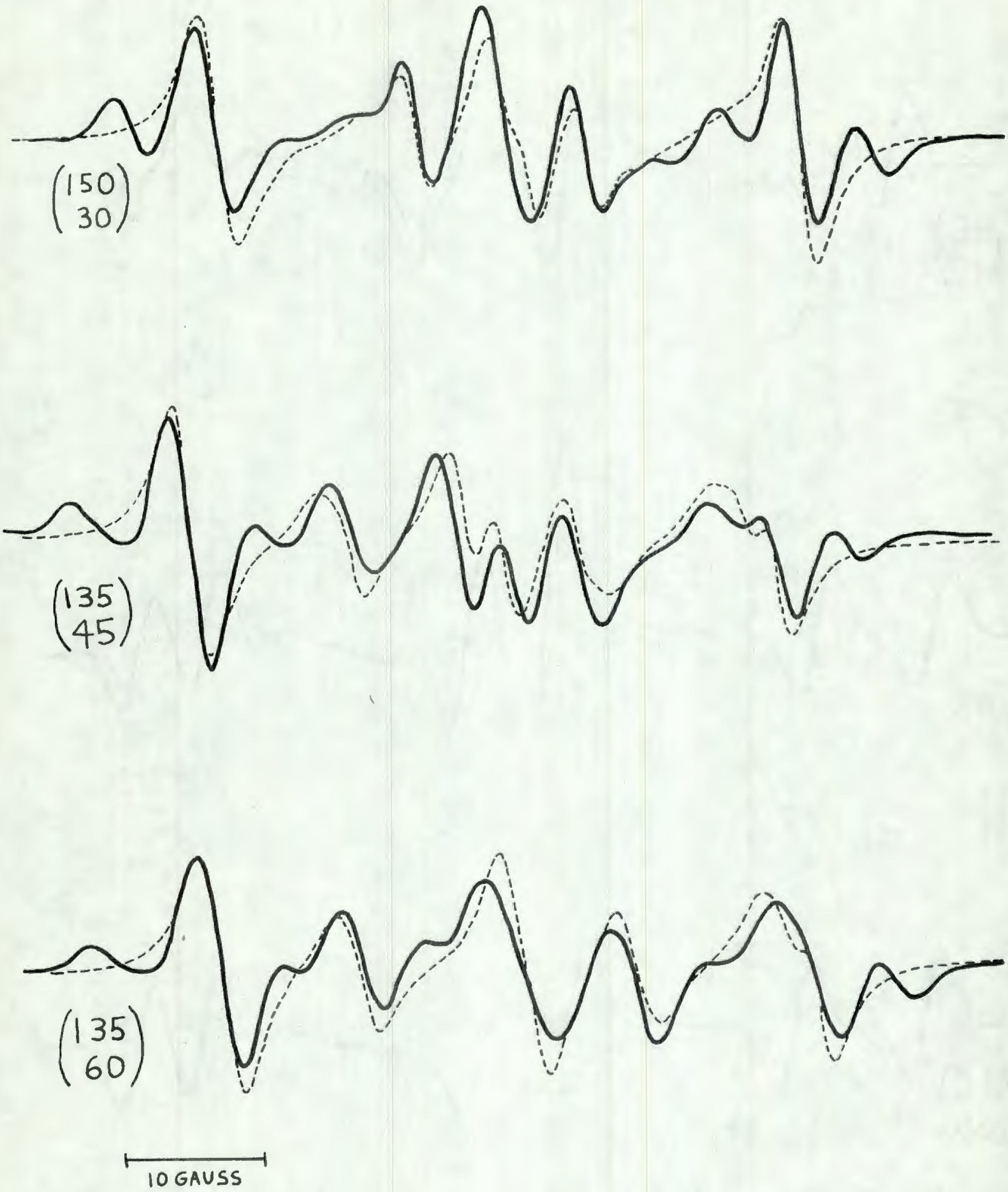
(150 30)
(135 45)
(135 60)
10 GAUSS

direction the coupling constants are very insensitive to change. Here the field vector is entering the plane perpendicular to the b axis where both sites are equivalent. Spectra taken with the field close to or along the b axis were the most sensitive to an error in ϕ. The effect of an error in θ on the coupling constants was found to be negligible.

The error in defining the center of each transition was estimated as ± .20 gauss which makes the total error estimate = ± .35 gauss. This is comparable to the standard deviation obtained in OPTIM.

4.1.4 Results

The parameters obtained using the data shown in Table I are listed below with the uncertainty calculated for each value:

Orientation of the $CH_2CO_2^-$ radical		Uncertainty
Twist	- 5.25°	.38
Wag	- 5.00°	.18
Flag	- 9.88°	.26
∠HCH	116.90°	.27
Principal Values of: H_1 Tensor		
	-26.80	.74
	-59.59	.44
	-92.15	.31
H_2 Tensor		
	-26.41	.99
	-58.98	.45
	-92.78	.20

Direction Cosines for:

H_1	(.547, .722, .423)
	(.768, -.634, .088)
	(- .332, -.276, .902)
H_2	(.048, -.081, -.996)
	(.768, -.634, .088)
	(.638, .769, -.032)

The direction cosines for H_1' and H_2' are related to the direction cosines for H_1 and H_2 by a 180° rotation about the b axis.

The smallest of the principal values for the coupling tensors reflected the largest uncertainties. These quantities represent the interaction along the C-H bonds.

Only ten of the thirteen parameters were determined with assurance that the parameters were actually independent. Using all 3 principal values of the g tensor as parameters gave erratic results. In evaluating the independence of only 2 g values as parameters a diagonalization was performed on the D'D matrix found in the least squares calculation which included the 2 g values as parameters. The large spread of the eigenvalues which resulted was indicative of questionable independence. This could have been avoided by choosing numbers of the same magnitude as the principal values of the coupling tensors and representing the g values in terms of these more appropriate numbers. However, a run was made using 12 parameters and the principal values of the g tensor became

$g_{xx} = 2.00242 \pm .00004$

$g_{yy} = 2.00353 \pm .00006$

$g_{zz} = 2.00420$ was fixed and not varied.

TABLE II. Parameters obtained from least squares fit.

PARAMETERS	1	2	3	4	5
Twist	- 4.79	- 5.26	- 5.25	- 6.30	- 5.18
Wag	- 4.79	- 5.00	- 5.00	- 5.35	- 5.14
Flap	- 9.86	- 9.88	- 9.88	- 9.64	- 9.95
HCH	116.77	116.90	116.90	116.72	116.79
PRINCIPAL VALUES					
H_1 Tensor					
	-26.93	-26.80	-26.80	-26.71	-26.17
	-59.48	-59.60	-59.59	-59.80	-59.29
	-92.24	-92.14	-92.15	-91.74	-92.52
H_2 Tensor					
	-25.75	-26.42	-26.41	-28.55	-26.17
	-60.06	-58.96	-58.98	-59.73	-59.29
	-92.37	-92.78	-92.78	-92.68	-92.52
g Tensor					
		2.00243			
		2.00354			
STANDARD DEVIATION					
	.417	.335	.335	.426	.339

Parameters obtained with

1. principal g values fixed at 2.0020, 2.0034, 2.0042 using 166 points for the least squares fit.
2. only 1 principal g value fixed; g_{zz} = 2.0042; used 166 points.
3. principal g values fixed at 2.00242, 2.00353, 2.00420; used 166 points.
4. Same as 3 except 244 points used for least squares fit.
5. assumption that coupling tensors are same; principal g values fixed at 2.00242, 2.00353, 2.00420; used 166 points.

These values were then used in a program varying only 10 parameters to obtain the best fit possible.

Due to different sets of data used and the number of parameters used for the least squares fit, the variation in the parameters was explored for these situations. The results are tabulated in Table II. One set of parameters was calculated using the assumption that both α-proton coupling tensors were the same. Table II also shows the use of all 6 principal values of the coupling tensor. The comparison of these parameters shows the validity of assuming that the coupling tensors are the same. The data taken for the 166 and 244 point programs was from the same spectra but the lowest number of points represents a refinement in this data. Differences were taken only between distinct and assignable lines. Overall the parameters are uniquely determined within experimental error. The standard deviation for each set of parameters obtained is included in Table II.

4.2 Spectrum of $CH_2CO_2^-$ radical

4.2.1 Observation of the "g-shift"

The basic spectrum for interaction of an electron with two inequivalent protons is a quartet with equal intensities (28). To illustrate the "g-shift", the spectra for 2 field orientations are shown in Figure 10. Under these spectra is plotted the stick spectrum obtained from the solution of the spin Hamiltonian in PREDICT. The upper spectrum was taken with the magnetic field perpendicular to the y axis (or b axis). Since the b axis was established as the two fold axis in the crystal the two magnetic

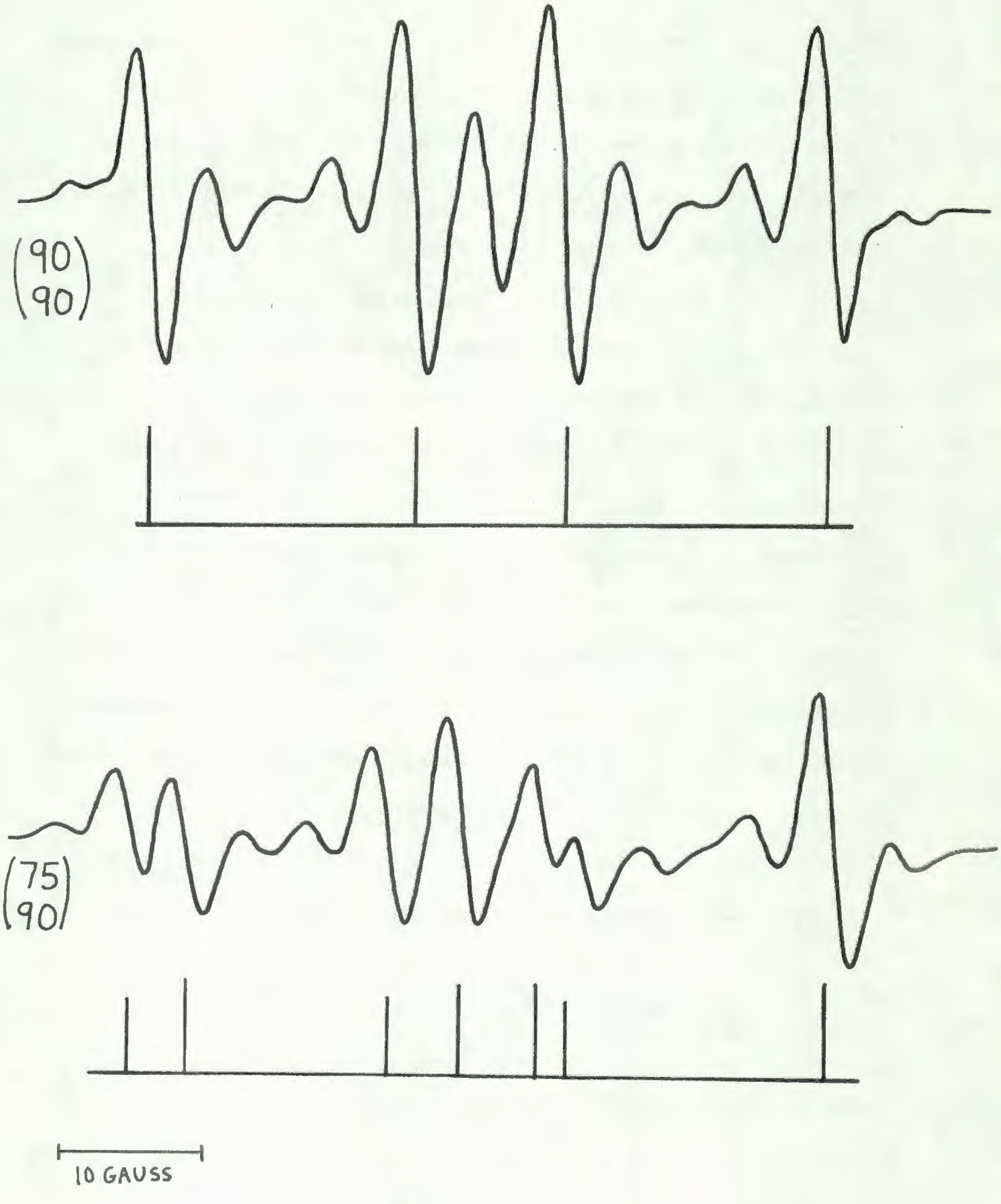

Figure 10. ESR spectra of the $\cdot CH_2CO_2^-$ radical at 133°K. Magnetic field parallel to b axis (top) and perpendicular to z axis in the x-y plane (bottom). Predicted stick spectrum plotted for comparison.

sites should be equivalent and the observed quartet agrees with this prediction (12). The coupling constants are the same for both sites. The lower spectrum was taken with the magnetic field perpendicular to the z axis and the effects of shifting each site due to existing anisotropies are apparent. All of the spectra taken perpendicular to the y axis exhibited the same characteristic of equivalent sites.

4.2.2 Symmetry of Inequivalent Sites

The stereographic net can again be used to demonstrate the symmetry present in a single crystal of $Zn(CH_3CO_2)_2 \cdot 2H_2O$. Referring to the Wulff net in Figure 6 it has already been mentioned that there are 79 different field orientations possible without duplicating spectra. If the right quadrant of the net is folded onto the left quadrant the spectra for these field directions will be the same but the sites will be interchanged. This is a result of the two fold symmetry about the b axis. And by the symmetry of a stereographic net the bottom half of the sphere is a replica of the top half. For a $\begin{pmatrix}45\\45\end{pmatrix}$ orientation the direction cosines were found to be (-.707,-.5, .5) by the following transformations

axis	D.C.
c	$\sin\theta\cos\phi$
b	$-\sin\theta\sin\phi$
a*	$-\cos\theta$

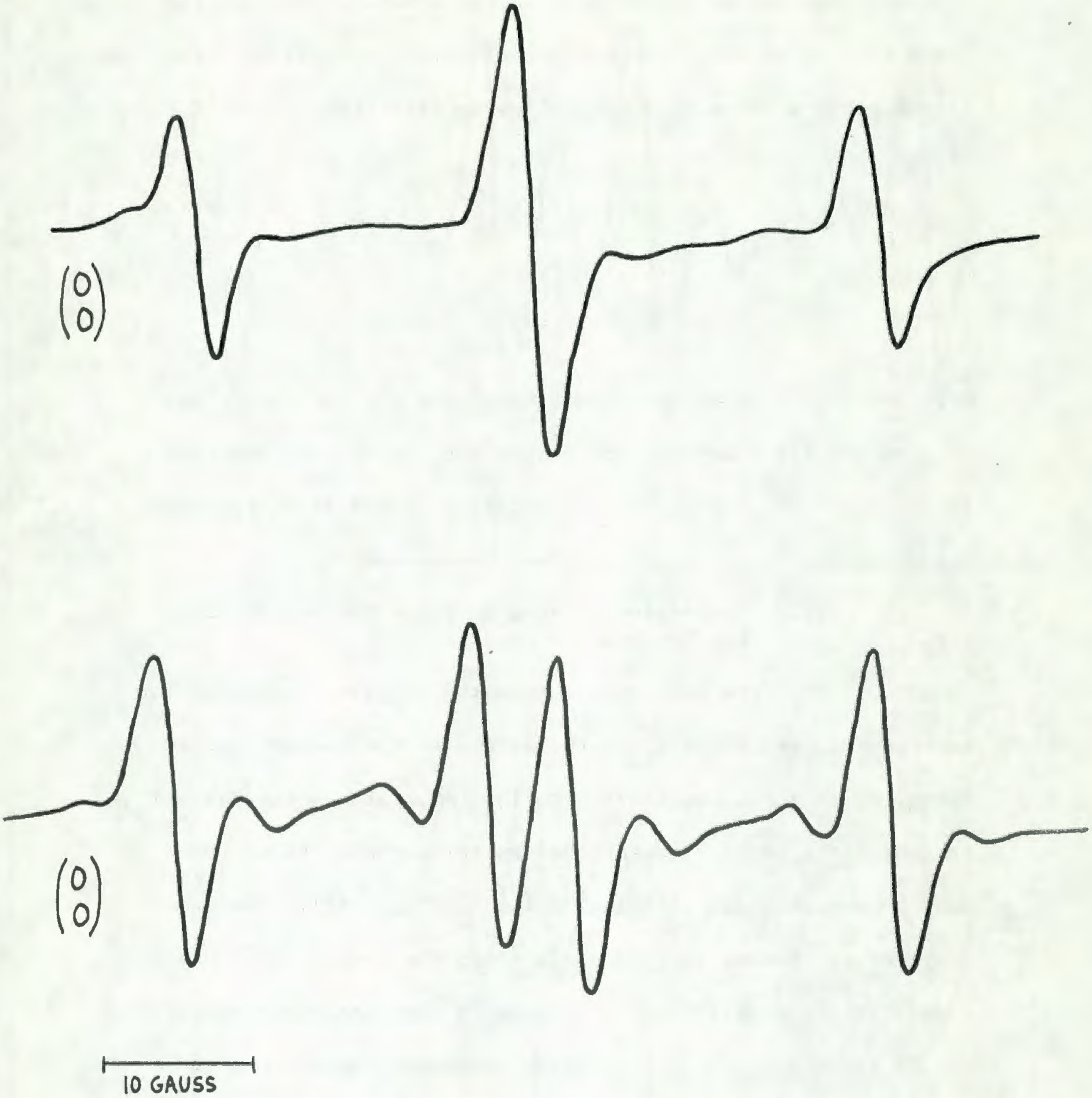

Figure 11. Comparison of ESR spectra of the $\cdot CH_2CO_2^-$ radical at room (top) and liquid nitrogen (bottom) temperature with magnetic field parallel to x axis.

These equations were direct results of the definitions of θ and Ø in the mounting of the crystal in section 3.4. The spectra taken with field direction cosines of (-.707,-.5,.5) were the same as the spectra taken with the following direction cosines for the field:

(+.707,+.5,-.5)
(-.707,+.5,+.5)
(+.707,-.5,-.5)

When only the sign of the direction cosine for the b axis was changed the sites were interchanged, but the spectra remained the same. This concept was particularly useful in manipulating the data.

4.2.3 Comparison of Room Temperature Spectra with Low Temperature Spectra

At room temperature the coupling constants for each proton were found to be the same with the magnetic field along the a* axis. On cooling to low temperatures the radical encountered a barrier to internal rotation about the C-C bond, and the center line split into 2 lines (Figure 11). The room temperature spectra for the field along the b axis also showed a triplet which split into a quartet on lowering the temperature to 133°K. The sum of the coupling constants for the 2 protons should be the same at low and high temperatures but these sums taken from the two spectra were not the same.

TABLE III. Changes in the sum of the coupling constants ($a_{H_1} + a_{H_2}$) for the methylene protons between room temperature and 133°K.*

Field Orientation	$a_{H_1} + a_{H_2}$ 298°K	$a_{H_1} + a_{H_2}$ 133°K	Change in $a_{H_1} + a_{H_2}$
$\begin{pmatrix}180\\0\end{pmatrix}$	45.3	47.5	2.2
$\begin{pmatrix}165\\0\end{pmatrix}$	42.0	44.1	2.1
$\begin{pmatrix}150\\0\end{pmatrix}$	38.9	41.7	2.8
$\begin{pmatrix}135\\0\end{pmatrix}$	36.8	40.6	3.8
$\begin{pmatrix}120\\0\end{pmatrix}$	36.6	40.7	4.1
$\begin{pmatrix}90\\90\end{pmatrix}$	44.5	47.7	3.2
$\begin{pmatrix}90\\75\end{pmatrix}$	40.0 48.5	42.6 51.1	2.6 2.6
$\begin{pmatrix}90\\45\end{pmatrix}$	34.8 49.2	40.6 52.7	5.8 3.5
$\begin{pmatrix}90\\15\end{pmatrix}$	36.9 44.2	38.7 46.0	1.8 1.8
$\begin{pmatrix}45\\30\end{pmatrix}$	44.7 51.8	45.4 55.9	.7 4.1
$\begin{pmatrix}60\\30\end{pmatrix}$	41.3 51.8	42.6 55.5	1.3 3.7
$\begin{pmatrix}75\\30\end{pmatrix}$	38.1 49.9	40.8 53.4	2.7 3.5
$\begin{pmatrix}45\\60\end{pmatrix}$	41.1 53.7	42.6 56.5	1.5 2.8

*For each field orientation ($a_{H_1} + a_{H_2}$) is given for both sites in the crystal.

Field Orientation	$a_{H_1} + a_{H_2}$ 298°K	$a_{H_1} + a_{H_2}$ 133°K	Change in $a_{H_1} + a_{H_2}$
$\begin{pmatrix}60\\60\end{pmatrix}$	38.8 53.7	41.7 56.8	2.9 3.1
$\begin{pmatrix}75\\60\end{pmatrix}$	37.3 52.1	41.0 55.4	3.7 3.3
$\begin{pmatrix}60\\75\end{pmatrix}$	39.7 51.3	41.9 55.3	2.2 4.0
$\begin{pmatrix}75\\75\end{pmatrix}$	39.5 50.3	41.5 53.5	2.0 3.2

Work has been done on the isotropic proton hyperfine interactions in the ESR of π-electron free radicals and it was concluded that out-of-plane vibrational motions should make a small contribution to the splitting as a result of the direct overlap between the proton and the unpaired electron in the π-orbital (28) (1). A contribution such as this would decrease with increasing temperature because of the relationship between the proton and electron spin with respect to out-of-plane vibrations. As out-of-plane vibrations increase, the sum of the coupling constants would then decrease. A theoretical analysis of the effect of vibrations on the methyl radical has been carried out by Schrader and Karplus (19). Zlochower, Miller, and Fraenkel applied this theory to the methyl radical and found a small dependence of hyperfine splitting with temperature (34) on the order of .04 gauss for a 20°C change in temperature in a 50°C range extending above and below room temperature. In this investigation a series of spectra taken at room temperature were compared with those at 133°K, and a change in hyperfine splitting of approximately 3 gauss was found. Some of these differences are tabulated in Table III for various field orientations.

4.2.4 Comparison of Calculated and Observed 2nd Order Lines

Suspected 2nd order lines were readily observed in spectra taken with the magnetic field perpendicular to the b and c axes. These lines were more intense with the field perpendicular to the b axis. Other directions of the magnetic field

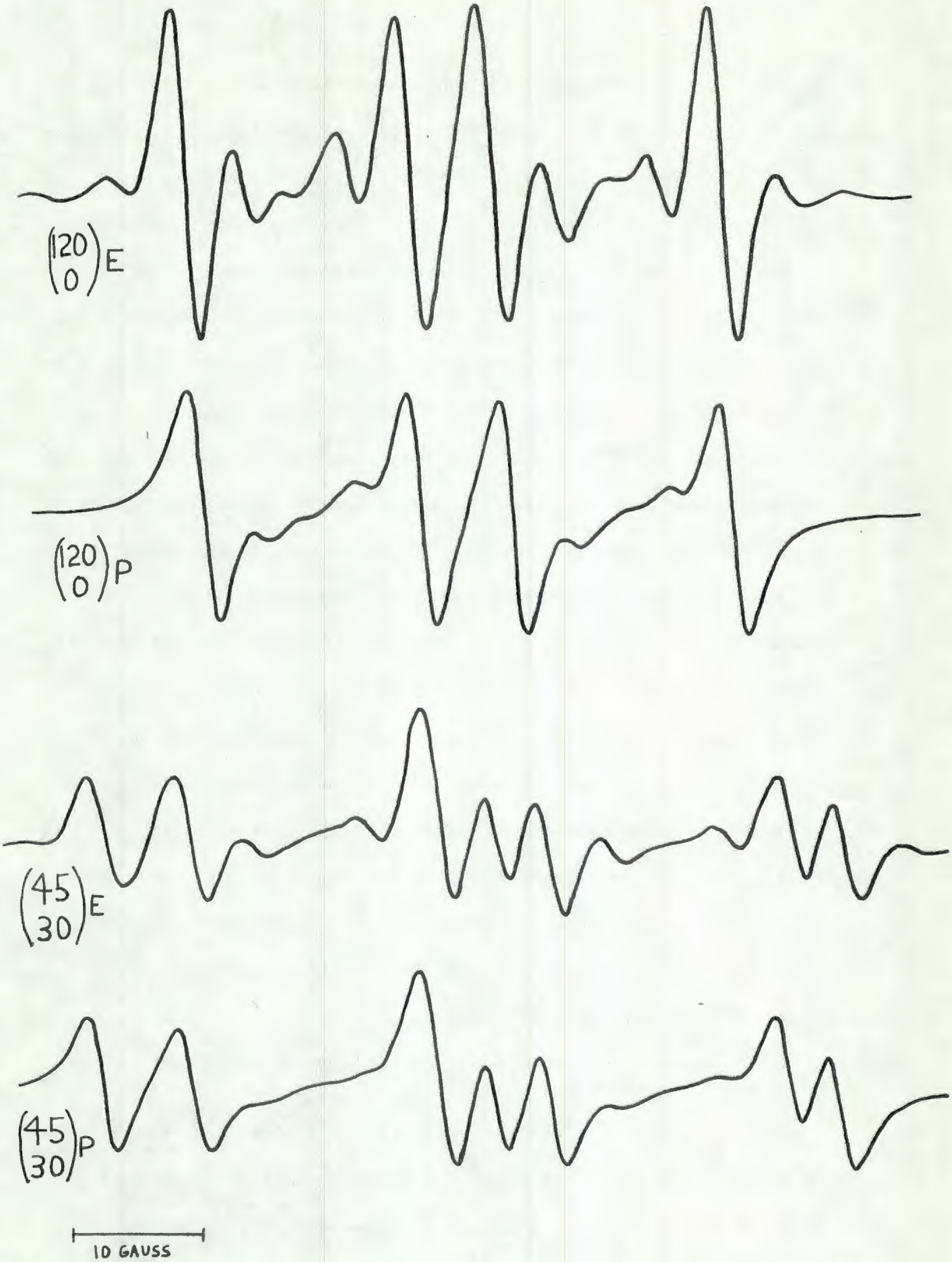

Figure 12. Experimental (E) and predicted (P) spectra of the $\cdot CH_2CO_2^-$ radical showing 2nd order lines.

resulted in such an overlap of the spectra from the two sites that the 2nd order lines were either buried by more intense lines or distorted by shoulder effects. Figure 12 shows experimental spectra in which 2nd order lines are observed. The spectra predicted by PREDICT were included below each experimental spectrum. The predicted 2nd order lines are not as intense and the experimental plot shows lines not predicted. Strangely enough, PREDICT computes practically no 2nd order lines for the (-,-,+) octant in the stereographic net while for nearly every orientation in the (+,-,+) octant, 2nd order lines are predicted with intensities ranging from .1 to .32 (relative to 1.0). The 45° bisector of this octant contains the orientations with the most intense 2nd order lines that were predicted.

4.2.5 Satellites

A D_2O substitution for H_2O was made in the zinc acetate in an effort to explain the appearance of satellite lines in the spectra (Figure 13). In an attempt to study similar satellites in irradiated sodium acetate trihydrate, Rogers and Kispert substituted D_2O for H_2O in the single crystal and observed a 6 fold reduction in satellite intensities (17).

The ESR spectra of irradiated $Zn(CH_3CO_2)_2 \cdot D_2O$ crystals were taken at $133^{\circ}K$ for selected orientations of the magnetic field (Figure 14). The crystals with D_2O were analyzed by NMR. A sample with only H_2O present resulted in an integrated peak of 88 mm and the sample with D_2O showed an integrated peak of 38 mm which included some OH fragments.

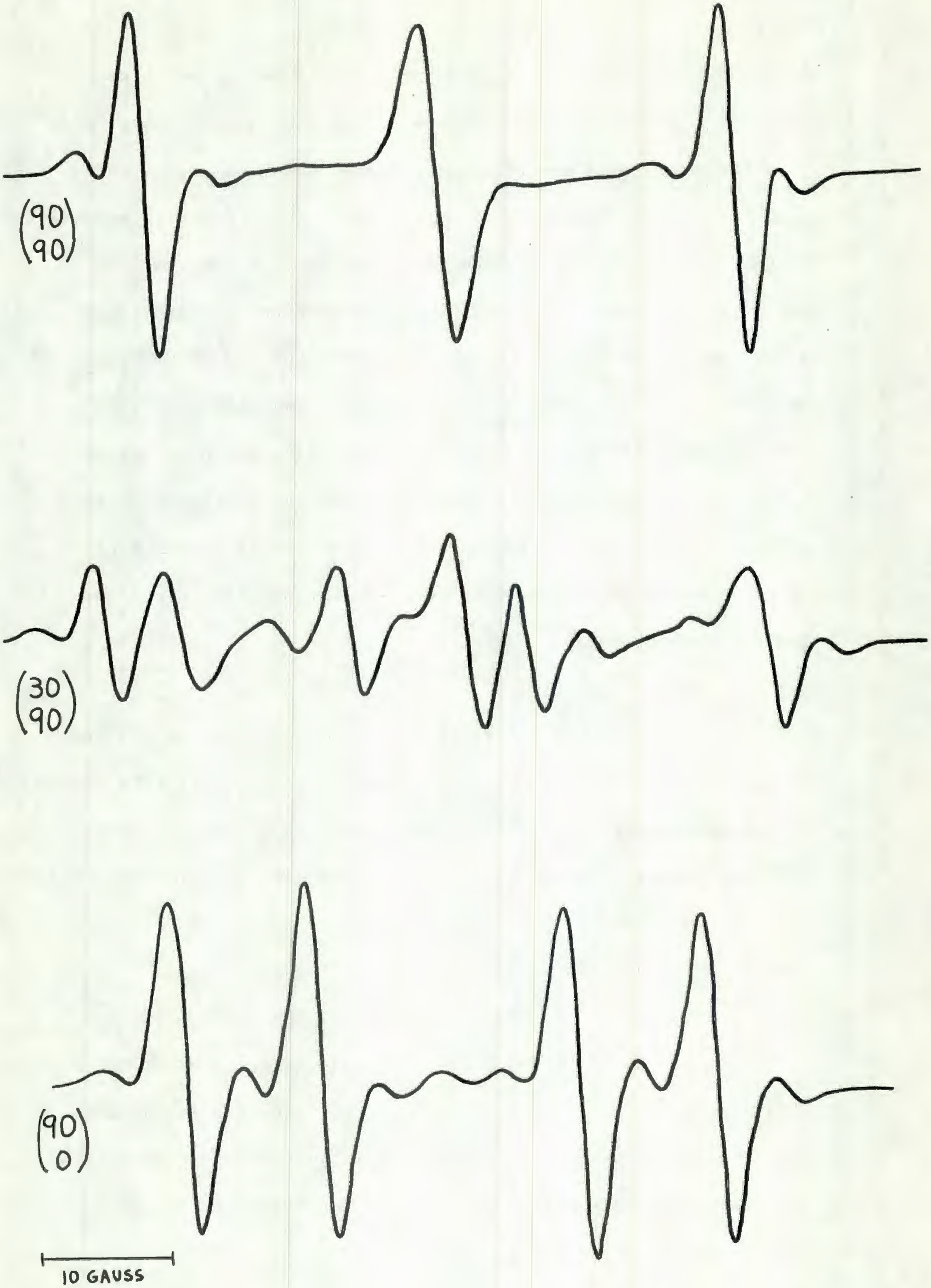

Figure 13. ESR spectra of the $\cdot CH_2CO_2^-$ radical. $\begin{pmatrix}90\\90\end{pmatrix}$ field direction at room temperature. Other spectra at $133^{\circ}K$.

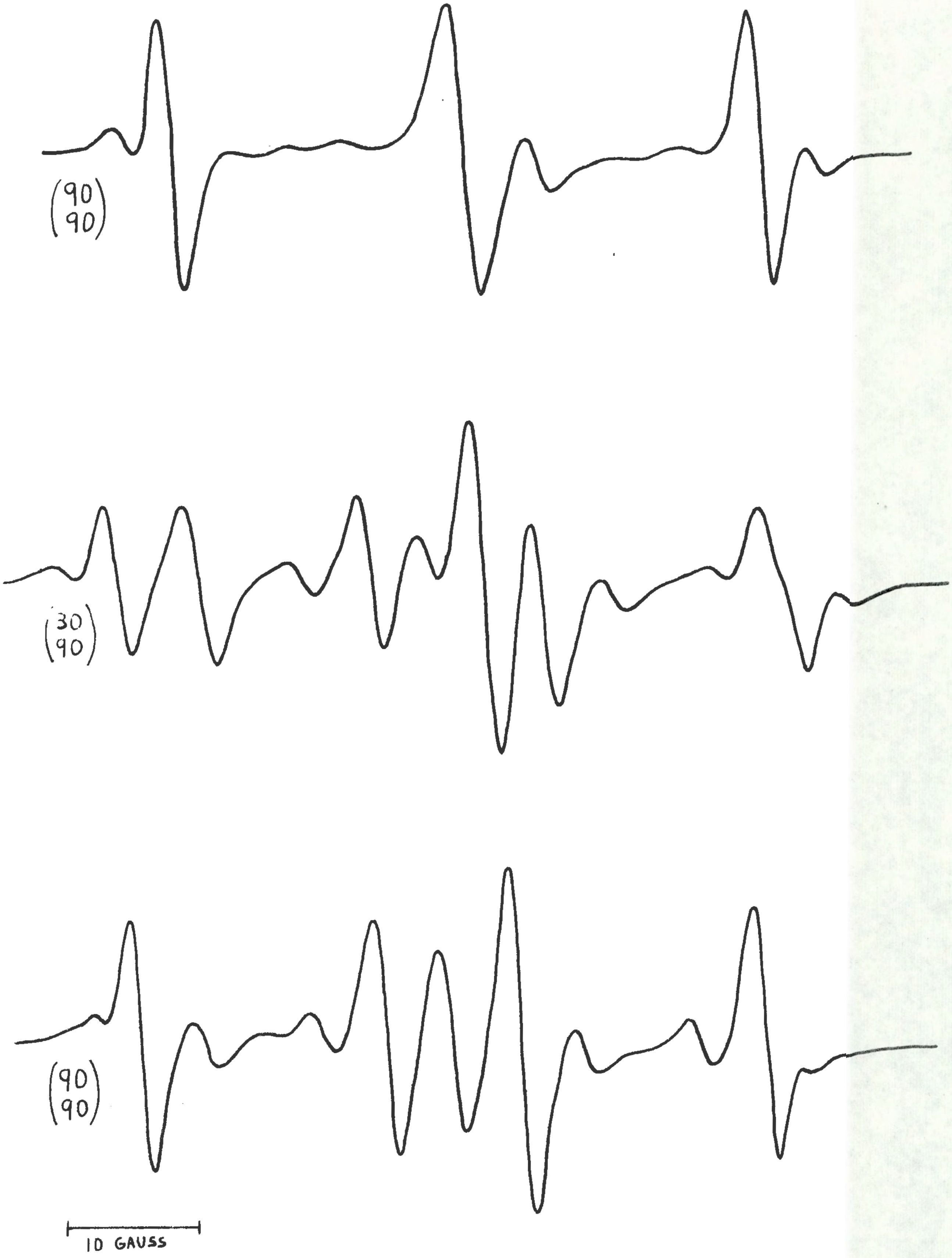

Figure 14. ESR spectra of $\cdot CH_2CO_2^-$ radical from irradiated single crystals of $Zn(CH_3CO_2)_2 \cdot D_2O$ taken at room temperature (top) and 133°K (bottom 2 spectra).

The spectra of the D_2O species were found to be identical to those without the D_2O substitution. One set of satellite lines are spaced approximately 5 gauss on either side of the main lines in both species. A second set of satellite lines are observed approximately 21 gauss from the main lines at high gain. The more intense satellite lines were found to increase in intensity at higher power but did not saturate. They appeared more prominent in spectra taken with the magnetic field positioned in the plane perpendicular to the two-fold axis. At these positions of the magnetic field the two sites were beginning to merge giving only one pattern for the two sites. Thus the satellite lines were less subject to shoulder effects and to dominance by the more intense lines of the quartet.

The satellites in sodium acetate trihydrate were finally attributed to "spin-flip" transitions (17), which arose when there was a simultaneous change in the spin state of the odd electron on the methyl radical and of neighboring protons. Analogous results were a possibility in this investigation with the odd electron located on the α-carbon of the methylene group and the spacing of the satellite lines occurring at a value close to the proton resonance frequency (5.0 to 5.8 gauss) in the magnetic field employed. Since no change in the spectra was observed using the D_2O substitution the neighboring protons that could be responsible for the spin flips would have to be located in a species oriented near the $\cdot CH_2CO_2^-$ radical. The protons of undamaged $CH_3CO_2^-$ were considered likely possibilities, but the most plausible theory in this investigation would be based on a spin flip of one proton concurrent with a spin flip of the unpaired electron.

Evidence of a single spin flip has also been observed in the spectra of gamma-irradiated single crystals of hydroxylated organic compounds (16) by Rao, et.al., using the theory of Trammel, Zeldes, and Livingston (27). This theory was applied in this investigation with a proton placed near the methylene group in the $\cdot CH_2CO_2^-$ radical but the resulting predictions were not altogether conclusive. The problems with shouldering effects, overlapping lines, and 2nd order lines were partially responsible for the unsuccessful analysis. And of course another species could be present making the assignment even more difficult.

4.3 Spectrum of Irradiated $Zn(CH_2DCO_2)_2 \cdot 2H_2O$

Spectra were taken at 133°K for selected field orientations since this investigation was primarily concerned with the isotope effect of a proton abstraction to form the $\cdot CHDCO_2^-$ radical. A spectrum for one field orientation is shown in Figure 15. By orienting the magnetic field perpendicular to the two-fold axis the g anisotropy was eliminated. This gave a spectrum that was easily comparable to a hyperfine pattern. A computer program was used to simulate the hyperfine pattern resulting from the substituted deuterium (24). The spectrum predicted by this program is also shown in Figure 15 to indicate the agreement obtained. The coupling constants taken from main line separations in the experimental spectrum compared favorably with those from spectra of the $\cdot CH_2CO_2^-$ radical for the same field orientation.

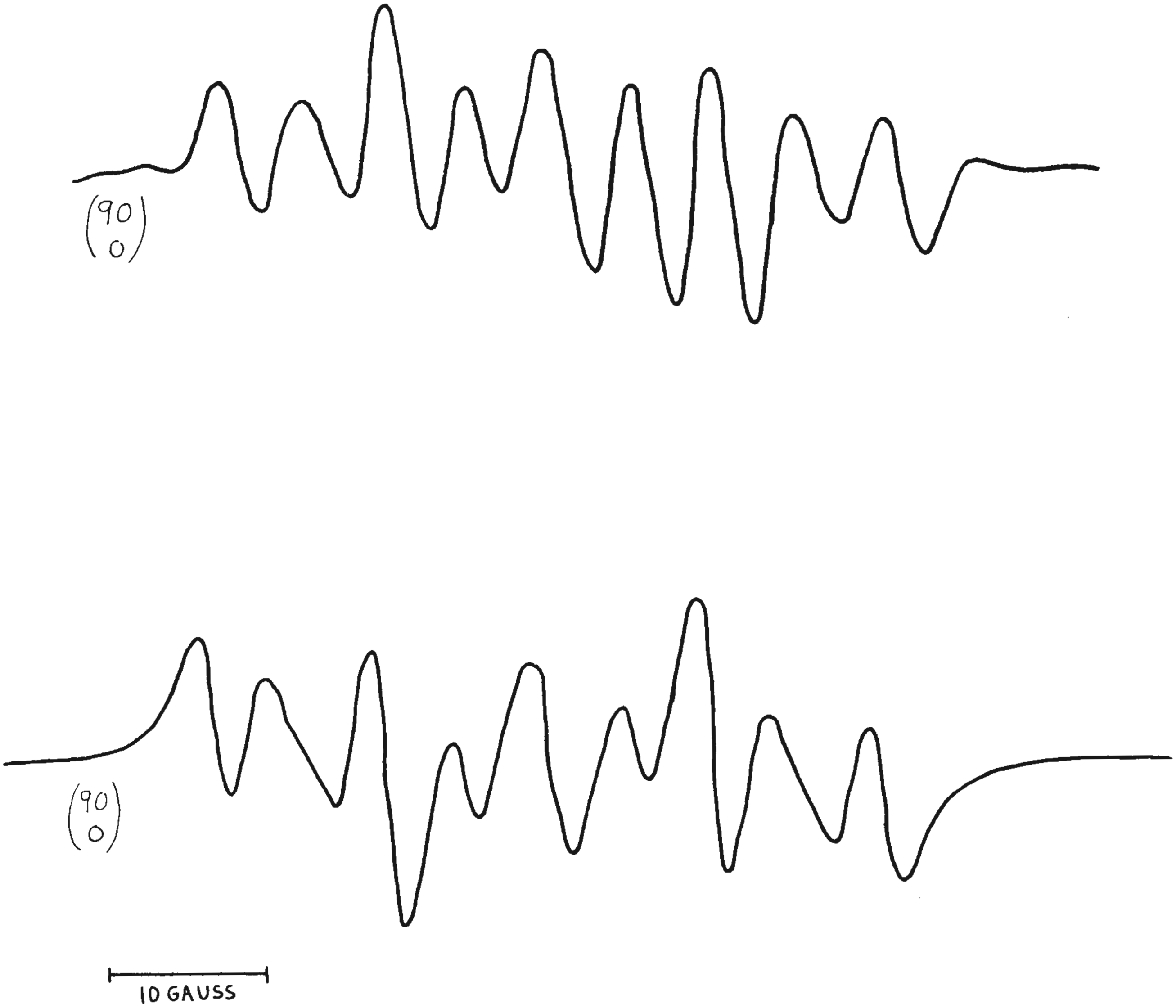

Figure 15. ESR spectrum of $CHDCO_2^-$ radical with magnetic field perpendicular to b axis. Bottom spectrum predicted assuming a 2:1 ratio of $CHDCO_2^-$: $CH_2CO_2^-$.

The hyperfine structure was predicted using the two radicals $CHDCO_2^-$ and $CH_2CO_2^-$ but realizing that $CHDCO_2^-$ radicals would exist as conformers. The coupling constant for deuterium was known to be .153 times that of hydrogen and since a deuteron may split each proton line into a triplet, the overlap of the lines in the center of the spectrum was to be expected. Also, this overlap was hard to interpret because of the presence of the CO_2^- radical in the center portion of the experimental spectra. However, the quartet from the $\cdot CH_2CO_2^-$ radical was easily identified and this formed a good basis of comparison between the predicted and experimental spectra.

In considering an isotope effect two mechanisms involving the formation of $\cdot CHDCO_2^-$ and $\cdot CH_2CO_2^-$ radicals were postulated. When a methyl radical (created by radiation damage) is located in a position close to an undamaged acetate ion, an isotope effect can exist; a C-H bond is more easily broken than a C-D bond so that the ensuing reaction

$$\dot{C}H_2D + CH_2DCO_2^- = CH_3D + \cdot CHDCO_2^-$$

results in formation of the $\cdot CHDCO_2^-$ radical. For a non-radical type reaction involving hydrogen and deuterium the maximum isotope effect has been reported as 6.9:1 (32). But with the methyl radical taking part in the reaction a large isotope effect is expected (31). If this is the case, the breaking of a C-H bond can be termed the barrier to formation of the radical. But the methyl radical may also migrate through the crystal until it approaches an acetate ion and randomly selects a hydrogen or deuterium. Thus a statistical basis is created when there is an equal probability of selection. The barrier to formation of the radical is then the migration of the methyl radical through the crystal. If the resulting abstractions are truly statistical two conformers of $\cdot CHDCO_2^-$ will be formed for each $\cdot CH_2CO_2^-$ radical. To show this statistical effect in the predicted hyperfine patterns, the intensities for each radical were adjusted on a quantitative basis. The quartet was assigned a relative intensity of 1 and the two conformers whose pattern consisted of 6 lines each were assigned a value of .67. Thus the sum of the intensities for each radical was 4 and the statistical ratio of 2:1 ($CHDCO_2^-$ over $\cdot CH_2CO_2^-$) was maintained. The agreement obtained between predicted and experimental hyperfine patterns was excellent but the statistical model used was based on 100% deuteration. An analysis using ESR intensities of the $\cdot CH_3$ radical vs the $\cdot CH_2D$ radical from spectra of irradiated Zn $(CH_2DCO_2)_2 \cdot 2H_2O$ at $113^{o}K$ showed only 79 $\pm$ 3% deuteration of the acetate ion. If there were only 79% $CH_2DCO_2^-$ and 21% $CH_3CO_2^-$ present initially, the resulting ratio of $CHDCO_2^-$: $CH_2CO_2^-$ would be 1.1:1 assuming the abstraction of a proton to be entirely satistical. But the experimental spectra still agreed with the predicted hyperfine pattern which assumed the 2:1 ratio. For a general approach:

$$\begin{array}{ccccc} CH_2DCO_2^- & \longrightarrow & CHDCO_2^- & + & CH_2CO_2^- \\ a & & b & & c \\ CH_3CO_2^- & \longrightarrow & & & CH_2CO_2^- \\ 1-a & & & & 1-a \end{array}$$

where $\frac{b}{2c}$ = isotope effect

$a = b + c$

But experimentally

$r = \frac{b}{1-a+c}$ ($r = 2.0 \pm .3$ in this investigation)

Solution:

$$\frac{b}{2c} = \frac{r}{2[r(a-1)+a]}$$

If $r = 2.0 \pm .3$

$a = .79 \pm .03$, then $\frac{b}{2c} = 3.0 \pm 1.0$

So there is a significant isotope effect and the barrier to formation of the $\cdot CH_2CO_2^-$ radical is the breaking of the C-H bond on the acetate ion. The methyl radical probably resides in a position near the acetate ion from which it abstracts a proton.

5. Molecular Orbital Calculation for the $CH_2CO_2^-$ Radical

In working with the $\cdot CH_2CO_2^-$ radical the spin density of the electron was assumed to be concentrated on the α-carbon. The results obtained in section 4 showed this to be correct. To verify this a molecular orbital calculation based on the CNDO approximation was made (25)(15). The spin density on the α-carbon for the planar radical was found to be .69 with each of the oxygens having a density of .15. The calculation for the perpendicular form of the radical yielded a spin density of .82 on the α-carbon. The value of .69 for the planar configuration necessitated a check on the spin density for the α-carbon of the $\cdot CH(COOH)_2$ radical because the principal values of the coupling tensor for this radical had been used as initial parameters in this investigation. The spin density on the α-carbon of the $\cdot CH(COOH)_2$ radical was calculated to be .66 and in good agreement with the planar configuration of the $\cdot CH_2CO_2^-$ radical.

The barrier to internal rotation of the methylene protons in the $\cdot CH_2CO_2^-$ radical was observed by Valenti and other investigators previously. The molecular orbital calculations on the planar and perpendicular models showed the planar form to be more stable. This degree of stability represents the barrier to internal rotation which turned out to be 11.8 kcal. The experimental value for the barrier has been calculated (using two different methods) to be 5.5 kcal (26). The difference between these values is somewhat attributed to the environment in the crystal, but the errors inherent in such a calculation must be considered also. Nevertheless, a large zinc atom is coordinating four formula units of the acetate in the crystal which makes the lattice a unique home for the $\cdot CH_2CO_2^-$ radical.

6. Conclusions

A positive identification of the $\cdot CH_2CO_2^-$ radical in an irradiated single crystal of zinc acetate dihydrate has been made. The orientation of the radical in the crystal has been determined with an HCH angle of $116.9^\circ \pm .3^\circ$. The radical's configuration is nearly planar, a result in agreement with other investigations (2) (22). The principal values of the A and g tensors were found to be of the same magnitude as tensors of other similar radicals in radiation damage studies. As in other π-electron radicals the spin density was found primarily on the α-carbon (20). A molecular orbital calculation supported this result and from the calculation the planar form of the radical was observed to be the stable configuration.

It has been observed in the comparison of spectra of irradiated single crystals of $Zn(CH_2DCO_2)_2 \cdot 2H_2O$ with predicted hyperfine patterns that a significant isotope effect exists. Proton abstractions from acetate ions by neighboring methyl radicals are considered the primary means for the formation of $\cdot CH_2CO_2^-$ radicals. The barrier to formation of the $\cdot CH_2CO_2^-$ radical is then the breaking of the C-H bond on the undamaged acetate ion.

A temperature dependence of the coupling constants for both methylene protons has been observed in spectra at $298^\circ K$ and $133^\circ K$. The magnitude of the coupling constants increases with decreasing temperature and at a rate approximately 10 times larger than the rate found by Zlochower and co-workers in their study of the methyl radical (34).

The satellites appear to be "spin-flip" transitions which arise from a change in the spin state of a proton on an undamaged acetate ion concurrent with a change in spin state of the electron on the α-carbon, but a further study of satellite line behavior is warranted. The D_2O substitution had no effect on the satellite lines; thus the water molecules are far enough removed from the unpaired electron to limit interactions and it is concluded that no dipole-dipole interaction takes place between the water and methylene protons of the $\cdot CH_2CO_2^-$ radical.

The 2nd order lines predicted by OPTIM are still not clearly assigned in the experimental spectra due to the confusion with possible spin flip satellites. There is some evidence from spectra taken perpendicular to the b axis that the intensities of the satellites are increased due to superposition with 2nd order lines.

BIBLIOGRAPHY

1. Anderson, D. H., Frank, P. J., and Gutowsky, H. S., J. Chem. Phys. 32, 196 (1960).

2. Box, H. C., Freund, H. G., and Budzinski, E. E., J. Am. Chem. Soc. 88, 658 (1966).

3. Carrington, A., and McLachlan, A. D., Introduction to Magnetic Resonance; Harper and Row, Inc., (1967).

4. Cochran, E. L., Adrian, F. J., and Bowers, V. A., J. Chem. Phys., 34, 1161 (1961).

5. Cole, T., J. Chem. Phys., 35, 1169 (1961).

6. Combrisson, J., and Uebersfeld, J., Compt. Rend., 238, 1397 (1954).

7. Cram, D. J., and Hammond, G. S., Organic Chemistry; McGraw-Hill, (1959).

8. Ghosh, D. K., and Whiffen, D. H., Mol. Phys., 2, 285 (1959).

9. Horsfield, A., Morton, J. R., and Whiffen, D. H., Mol. Phys., 4, 327 (1961).

10. Marmor, S., Laboratory Guide for Organic Chemistry; Heath, (1964).

11. McConnell, H. M., Heller, C., Cole, T., and Fessenden, R. W., J. Am. Chem. Soc., 82, 766 (1960).

12. Morton, J. R., Chem. Rev., 64, 453 (1964).

13. Morton, J. R., J. Am. Chem. Soc., 86, 2325 (1964).

14. Pake, G. E., Towsend, J., and Weissman, S. I., Phys. Rev., 85, 682 (1952).

15. Pople, J. A., and Segal, G. A., J. Chem. Phys. 43, 5136 (1965).

16. Rao, M. J., and Anderson, R. S., J. Chem. Phys. 42, 2899 (1965).

17. Rogers, M. T., and Kispert, L. D., J. Chem. Phys., 46, 221 (1967).

18. Schoening, F. R. L., van Niekerk, J. N., and Talbot, J. H., Acta Cryst., 6, 720 (1953).

19. Schrader, P. M., and Karplus, M., J. Chem. Phys., 40, 1593 (1964).

20. Shrivastava, K. N., and Anderson, R. S., Abstract, Meeting of the American Physical Society, Boston, Mass., Feb. 1968, No. AC12.

21. Slichter, C. P., Principles of Magnetic Resonance; Harper and Row, Inc., (1963).

22. Smith, P., Pearson, J. T., Wood, P. B., and Smith, T. C., J. Chem. Phys., 43, 1535 (1965).

23. Toles, W. M., A Computer Program for Prediction of ESR Spectra using Isotropic g and Hyperfine Coupling Tensors for Protons, unpublished.

24. Tolles, W. M., A Computer Program for Prediction of the Hyperfine Structure of a Radical, unpublished.

25. Tolles, W. M., A Computer Program for Molecular Orbital Calculations using the CNDO Approximation, unpublished.

26. Tolles, W. M., unpublished.

27. Trammell, G. T., Zeldes, H., and Livingston, R., Phys. Rev., 410, 630 (1958).

28. Valenti, J. L., Electron Spin Resonance Study of Free Radical Formation in Irradiated Zinc Acetate Dihydrate, (Thesis) USNPGS, (1967).

29. Venkataraman, B., and Fraenkel, G. K., J. Chem. Phys., 24, 737 (1956).

30. Weiner, R. F., and Koski, W. S., J. Am. Chem. Soc., 85, 853 (1963).

31. Wiberg, K. B., Chem. Rev., 55, 713 (1955).

32. Wiberg, K. B., Physical Organic Chemistry; John Wiley and Sons, Inc., (1964).

33. Wilkinson, J. H., The Algebraic Eigenvalue Problem; Clarendon Press, Oxford (1965).

34. Zlochower, I. A., Miller, W. R., and Fraenkel, G. K., Letter to the Editor, J. Chem. Phys., 42, 3339 (1965).

APPENDIX I

A computer program for calculating transition frequencies and intensities for radicals oriented in a crystal lattice. The program is written in Fortran IV for use with the IBM 360 computer.

```
C
C     PROGRAM PREDICT
C
C   NN IS THE NUMBER OF SPIN = .5 NUCLEI TO BE INCLUDED IN THE CALCULATION
C   IFRPT IS ZERO FOR INITIAL SET OF DIRECTION COSINES, THEN NOT ZERO FOR EACH
C     REPEATED CALCULATION TO BE DONE BY JUST CHANGING THE DIRECTION COSINES
C     OF THE MAGNETIC FIELD
C   H IS THE MAGNITUDE OF THE MAGNETIC FIELD, MEASURED IN MEGACYCLES OF THE
C     NUCLEAR ZEEMAN FREQUENCY
C   DCOS IS THE DIRECTION COSINES MATRIX.  ELEMENT I,J,K IS FOR NUCLEUS I,
C     RELATING THE J-TH PRINCIPAL AXIS WITH THE KTH CRYSTAL AXIS
C   A(I,J) IS THE J-TH PRINCIPAL VALUE OF THE COUPLING TENSOR FOR ATOM I
C   UH(I) IS THE I-TH COMPONENT OF THE UNIT VECTOR POINTING ALONG THE
C        DIRECTION OF THE MAGNETIC FIELD
C   DE IS THE ARRAY OF TRANSITION FREQUENCIES CALCULATED
C   FINT IS THE CORRESPONDING ARRAY OF INTENSITIES
C   IC IS THE NUMBER OF TRANSITIONS CALCULATED
C
      DIMENSION DCOS(10,3,3), A(10,3), UH(3), DE(1000), FINT(1000)
    1 READ(5,100) NN,IFRPT,H
      IF(IFRPT) 5,5,20
    5 IF(NN) 1000,1000,10
   10 DO 15 I = 1,NN
   15 READ(5,101) ((DCOS(I,J,K), K = 1,3), J = 1,3)
      DO 16 I = 1,NN
   16 READ(5,102) (A(I,J), J = 1,3)
   20 READ(5,103) (UH(I), I = 1,3)
      IF(IFRPT) 25,25,40
   25 WRITE (6,111) H
      WRITE(6,104)
      DO 30 I = 1,NN
   30 WRITE (6,105) ((DCOS(I,J,K), K = 1,3), J = 1,3)
      WRITE(6,106)
      DO 31 I = 1,NN
   31 WRITE(6,107) (A(I,J), J = 1,3)
   40 WRITE(6,108) (UH(I), I = 1,3)
      CALL SSESR(NN,DCOS,A,UH,H,DE,FINT,IC)
      WRITE(6,109) (DE(I), I = 1,IC)
      WRITE(6,110) (FINT(I), I = 1,IC)
      DO 50 I = 1,IC
   50 DE(I) = DE(I)/2.80246
      WRITE(6,112) (DE(I), I = 1,IC)
      GO TO 1
 1000 STOP
  100 FORMAT(I2,I3,F10.5)
  101 FORMAT (9F7.5)
  102 FORMAT (3F7.3)
  103 FORMAT (3F7.5)
  104 FORMAT (1X,//' DIRECTION COSINES'//)
  105 FORMAT (1X,9F12.7)
  106 FORMAT (1X,//' COUPLING CONSTANTS'//)
  107 FORMAT (1X,3F10.5)
  108 FORMAT (1X,/////' DIRECTION COSINES FOR H',//(3F12.7)//)
  109 FORMAT (1X,' TRANSITION FREQUENCIES',/(10F11.5))
  110 FORMAT (1X,' TRANSITION INTENSITIES',/(10F11.5))
  111 FORMAT ((1H1,'NUCLEAR ZEEMAN FREQUENCY = 'F11.5)//)
  112 FORMAT (//' TRANSITIONS, IN GAUSS FROM CENTER, ASSUMING G = 2.0023
     1',/(10F11.5))
      END
C
C
C
C
      SUBROUTINE SSESR(NN,DCOS,A,UH,H,DE,FINT,IC)
C  NN IS THE NUMBER OF NUCLEI WITH SPIN = .5
C  DCOS IS THE DIRECTION COSINE MATRIX.  ELEMENT I,J,K RELATES THE COMPONENT
C    FOR ATOM I OF THE J-TH PRINCIPAL AXIS ALONG THE K-TH CRYSTAL AXIS
C  A(I,J) IS THE J-TH PRINCIPAL VALUE FOR THE I-TH ATOM
C  UH(I) IS THE I-TH COMPONENT OF THE UNIT VECTOR POINTING ALONG THE
C      DIRECTION OF THE MAGNETIC FIELD
C  DE IS THE ARRAY OF TRANSITION FREQUENCIES CALCULATED
C  FINT IS THE CORRESPONDING ARRAY OF INTENSITIES
C  IC IS THE NUMBER OF TRANSITIONS CALCULATED
      DIMENSION DCOS(10,3,3), A(10,3), UH(3), DE(1000), FINT(1000),
     1HV(10,3), HVP(10,2,3), CE(10), HCOS(10,3), ABH(10,2), S(2), IQ(20)
      S(1) = 1.0
      S(2) = -1.0
      DO 10 I = 1,NN
      DO 10 J = 1,3
      HCOS(I,J) = 0.0
      DO 10 K = 1,3
   10 HCOS(I,J) = HCOS(I,J)+UH(K)*DCOS(I,J,K)
      WRITE(6,100) ((HCOS(I,J), J = 1,3), I = 1,NN)
      DO 15 I = 1,NN
      DO 15 J = 1,3
   15 HV(I,J) = 0.0
      DO 20 I = 1,NN
      DO 20 J = 1,3
      CAS = HCOS(I,J)*A(I,J)
      DO 20 K = 1,3
   20 HV(I,K) = HV(I,K) + CAS*DCOS(I,J,K)
      WRITE(6,100) ((HV(I,J), J = 1,3), I = 1,NN)
      DO 30 I = 1,NN
      DO 30 J = 1,2
      DO 30 K = 1,3
   30 HVP(I,J,K) = H*UH(K)-0.5*S(J)*HV(I,K)
      WRITE(6,100) (((HVP(I,J,K), K = 1,3), J = 1,2), I = 1,NN)
      DO 40 I = 1,NN
      DO 40 J = 1,2
      ABH(I,J) = 0.0
      DO 35 K = 1,3
   35 ABH(I,J) = ABH(I,J) + HVP(I,J,K)**2
   40 ABH(I,J) = SQRT(ABH(I,J))
      WRITE(6,100) ((ABH(I,J), J = 1,2), I = 1,NN)
      DO 50 I = 1,NN
      CE(I) = 0.0
      DO 45 J = 1,3
   45 CE(I) = CE(I) + HVP(I,1,J)*HVP(I,2,J)
   50 CE(I) = CE(I)/(ABH(I,1)*ABH(I,2))
      WRITE(6,100) (CE(I), I = 1,NN)
      NN2 = 2*NN
      NNTT = 2**(2*NN)
      HNNT = 2**NN
      DO 55 I = 1,NN2
   55 IQ(I) = 1
      IC = 0
      DO 70 I = 1,NNTT
      IC = IC+1
      DE(IC) = 0.0
      FINT(IC) = 1.0
      DO 60 J = 1,NN
      J1 = IQ(J)
      J2 = IQ(NN+J)
      FINT(IC) = FINT(IC)*(1.0-S(J1)*S(J2)*CE(J))
   60 DE(IC) = DE(IC) + S(J1)*ABH(J,1) + S(J2)*ABH(J,2)
      DE(IC) = 0.5*DE(IC)
      FINT(IC) = FINT(IC)/HNNT
      J = 1
   64 IF(IQ(J)-2) 66,65,66
   65 IQ(J) = 1
      J = J+1
      GO TO 64
   66 IQ(J) = 2
   70 CONTINUE
  100 FORMAT (1H ,10F11.5)
```

```
      RETURN
      END
C
C   AN EXAMPLE OF THE DATA IS AS FOLLOWS
C
 2     36.46
 -631    299   -715    191    955    227   -753   -011    659
  968   -141   -213    191    955    227    170   -265    949
  290    610    910
  290    610    910
               1.0
 2  1  36.46
  70711         70711
 2  1  36.46
  966           259
 2  1  36.46
  86602        -50000
 2  1  36.46
  70711        -70711
 2  1  36.46
        1.0
 1    13.8
  21183  76829  60402 -97091  09484  21985  11162 -63303  76604
  30     60     90
 1
 1  1 13.8
        1
 1  1 13.8
               1
 1  1 13.8
  70711  70711
 1  1 13.8
  70711         70711
 1  1 13.8
         70711  70711
 1  1 13.8
  34202  93967
 1  1 13.8
  93967  34202
 1  1 13.8
  34202         93967
 1  1 13.8
  93967         34202
 1  1 13.8
         34202  93967
```

APPENDIX II

A computer program which performs a least squares fit on selected data from predicted and observed spectra for a radical oriented in crystal space. Differences between predicted frequencies are compared with the differences between observed frequencies and the least squares fit results in the determination of certain selected parameters. The program is written in Fortran IV for use with the IBM 360 computer.

```
C   PROGRAM OPTIM
C
C   THIS PROGRAM WILL CALCULATE ESR TRANSITION FREQS AND INTENS FOR AN
C   ORIENTED RADICAL IN A DEFINED CRYSTAL SYSTEM GIVEN THE PRINCIPAL
C   VALUES OF THE A AND G TENSORS.  IT WILL PERFORM A LEAST SQUARES FIT
C   ON DIFFS TAKEN BETWEEN SELECTED FREQS FOR OBSERVED AND CALCULATED
C   SPECTRA.  THE PARAMETERS ARE CORRECTLY DETERMINED BY THE LEAST
C   SQUARES FIT.
C
      IMPLICIT REAL*8(A-H,O-Z)
      DIMENSION ACOS(2,3,3),A(2,3),UH(3),DE(16),FINT(16),PAR(13),
     1 CC(3),HH(3),UHM(70,3),DEOB(250),IFS(70,13),R(250),
     2DT(13,250),DEL(13),PARN(13),DE1(250),DE2(250),B(2,3),DEN(13),
     3IR(70),DECOS(2,3,3),GCOS(2,3,3),GECOS(2,3,3),G(2,3),DEE(16),
     4DE4(250),DE3(250),DE5(250),DE6(250),G1(2,3),NFR(70),FINTE(16)
     5,IFE(70,13),NFRE(70)
     6,ID(60),LGR(70),IFM(70,13),IFN(70,13),IS(70)
     7,IT(70)
      REAL D(32),FIN(32),YI,ZI(60)
      REAL*8 ITITLE(12)
C
C   READ IN --- NN = NO. OF PROTONS(NN MAX = 2)
C               H - NUCLEAR ZEEMAN FREQ
C               DEN = THE INCREMENTAL CHANGE IN THE PARAMETERS
C                     USED TO OBTAIN THE NUMERICAL DERIVATIVES.
C
      READ(5,100) NN,H,DEN
C
C   READ IN --- CC & HH = DIRECTION COSINES FOR VECTORS ON WHICH
C                         INITIAL ORIENTATION OF RADICAL IS CONSTRUCTED.
C
      READ(5,114) CC,HH
C
C   READ IN --- PAR = INITIAL PARAMETERS
C
      READ(5,113)(PAR(I),I=1,13)
      WRITE(6,111) H
C
C   THE NEXT TWO ARRAYS ARE FOR SUBROUTINE SPEC
C   READ IN --- ID - CONTROLS NO. OF SPECTRA DRAWN ON EACH GRAPH.
C               ZI - CONTROLS THE SPACING OF THE SPECTRA ON EACH GRAPH.
C
      READ(5,126)(ID(I),I=1,60)
      READ(5,128)(ZI(I),I=1,60)
C
```

```
C     NOW BEGIN ITERATION PROCEDURE
C
C     READ IN --- NFLP = NO. OF MAGNETIC FIELD DIRECTIONS
C                 NP = NO. OF PARAMETERS OR VARIABLES FOR LEAST SQUARES
C                      FIT
C                 IP = INDEX WHICH IF = 0 READS IN NEW SET OF
C                      PARAMETERS AT END OF DATA AND IF = 1 PROCEEDS
C                      WITH ORIGINAL SET READ IN ABOVE
C
      1 READ(5,117) NFLP,NP,IP
        READ(5,15)(ITITLE(I),I=1,12)
C
C     READ IN THE NEXT THREE ARRAYS TO TELL THE COMPUTER HOW MANY
C     FREQS (BETWEEN WHICH DIFFS WILL BE TAKEN) HAVE BEEN SELECTED
C     FROM EACH SPECTRUM
C
C                 NFR  SITE 1
C                 NFRE  SITE 2
C                 LGR  SITE 1 & SITE 2
C
        READ(5,117)(NFR(I),I=1,NFLP)
        READ(5,117)(NFRE(I),I=1,NFLP)
        READ(5,117)(LGR(I),I=1,NFLP)
C
C     READ IN THREE MORE ARRAYS TO TELL COMPUTER TO INCLUDE (1)
C     OR EXCLUDE (0) A PARTICULAR SITE FOR  FREQ SELECTIONS
C                 IT    SITE 1
C                 IR    SITE 2
C                 IS    SITES 1 & 2
C
        READ(5,117)(IT(I),I=1,NFLP)
        READ(5,117)(IR(I),I=1,NFLP)
        READ(5,117)(IS(I),I=1,NFLP)
        NF2=0.0
        J1=1.0
        DO 200 I=1,NFLP
        NFE=NFRE(I)
        LG=LGR(I)
        NF=NFR(I)
        NF1=IT(I)*(NF-1)+IR(I)*(NFE-1)+IS(I)*LG
        NF2=NF2+NF1
C
C     UHM = MAGNETIC FIELD VECTORS
C
        READ(5,103)(UHM(I,J),J=1,3)
```

```
C
C   READ IN ARRAYS IFS,IFE,IFM, IFN TO INDICATE WHICH FREQS TO
C   SELECT WITHIN EACH SITE.  IFM AND IFN  FREQS ARE PAIRED FOR
C   DIFFS BETWEEN EACH SITE.
C               IFS   SITE 1
C               IFE   SITE 2
C               IFM   SITE 1
C               IFN   SITE 2
C
      READ(5,126) (IFS(I,J),J=1,NF)
      READ(5,126)(IFE(I,J),J=1,NFE)
      READ(5,126)(IFM(I,J),J=1,LG)
      READ(5,126)(IFN(I,J),J=1,LG)
C
C   READ IN EXPERIMENTAL DIFFS TO COMPARE WITH CALC FREQS.
C
      READ(5,113)(DEOB(J),J=J1,NF2)
      WRITE(6,108)(UHM(I,J),J=1,3)
      WRITE(6,113)(DEOB(J),J=J1,NF2)
      WRITE(6,129) NF2
      WRITE(6,118) NF1,I
  200 J1=J1+NF1
      IF(IP) 2,2,3
    2 READ(5,113)(PAR(I),I=1,13)
      WRITE(6,116)(PAR(N),N=1,NP)
    3 CONTINUE
      WRITE(6,115)(PAR(I),I=1,NP)
C
C   START ITERATION FOR LEAST SQUARES FIT.
C
      DO 60 M=1,3
      WRITE(6,106)
      DO 16 J=1,3
      J4=J+4
      J7=J+7
      J10=J+10
      A(1,J)=PAR(J4)
      A(2,J)=PAR(J7)
   16 G(1,J)=PAR(J10)
      DO 31 I = 1,NN
   31 WRITE(6,107) (A(I,J), J = 1,3)
      WRITE(6,124)(G(1,J),J=1,3)
C
C   ENTER TWSF TO UPDATE DIRECTION COSINES FOR EXISTING PARAMETERS.
C
```

```
      CALL TWSF(CC,HH,ACOS,DECOS,GCOS,GECOS,PAR)
      WRITE(6,104)
      DO 30 I = 1,NN
   30 WRITE (6,105) ((ACOS(I,J,K), K = 1,3), J = 1,3)
      DO 33 I=1,NN
   33 WRITE(6,105)((DECOS(I,J,K),K=1,3),J=1,3)
      WRITE(6,125)((GCOS(1,J,K),K=1,3),J=1,3)
      WRITE(6,125)((GECOS(1,J,K),K=1,3),J=1,3)
      LL=1
      L=1
      JJ=1
      KK=1
      DO 20 J=1,NFLP
      DO 35 K=1,3
   35 UH(K)=UHM(J,K)
C
C    ENTER SSESR TWICE FOR PREDICTED FREQS AND INTENS. FOR BOTH
C    SITES(MONOCLINIC CRYSTAL)
C
      CALL SSESR(NN,ACOS,GCOS,A,G,UH,H,DE,GEF,FINT,IC)
      CALL SSESR(NN,DECOS,GECOS,A,G,UH,H,DEE,GEFE,FINTE,IC)
      IX=1
      DO 36 I=1,IC
      D(IX)=DEE(I)
      FIN(IX)=FINTE(I)
      IX=IX+1
      D(IX)=DE(I)
      FIN(IX)=FINT(I)
   36 IX=IX+1
      NF=NFR(J)
      MODCUR=ID(J)
      YI=ZI(J)
C
C    IF DESIRED ENTER SPEC ON SELECTED ITERATION (M) FOR DRAWING
C    PREDICTED SPECTRA
C
      IF(M-4) 38,37,38
   37 CALL SPEC(ITITLE,D,FIN,IC,MODCUR,YI)
   38 CONTINUE
C
C    BEGIN FREQ SELECTION FROM EACH SITE
C
      DO 40 K=1,NF
      MM=IFS(J,K)
      DE1(L)=DE(MM)
   40 L=L+1
      NFE=NFRE(J)
      DO 41 K=1,NFE
      MM=IFE(J,K)
      DE3(JJ)=DEE(MM)
   41 JJ=JJ+1
      LG=LGR(J)
      DO 42 K=1,LG
      MM=IFM(J,K)
      KL=IFN(J,K)
      DE2(KK)=DE(MM)
      DE5(KK)=DEE(KL)
   42 KK=KK+1
      LGF=KK-LG
      K1=KK-1
      LNE=JJ-NFE
      LE=JJ-1
      LNF=L-NF
      LM=L-1
      I1=LNF+1
      I2=LNE+1
C
C   TAKE DIFFERENCES FROM SELECTED FREQS FOR SELECTED SITES AND
C   STORE UNTIL CALCS USING ALL FIELD VECTORS ARE COMPLETE
C
      IF(IT(J)) 47,47,48
   48 CONTINUE
      DO 410 N=I1,LM
      DE4(LL)=DABS(DE1(LNF)-DE1(N))
  410 LL=LL+1
   47 CONTINUE
      IF(IR(J)) 46,46,45
   45 CONTINUE
      DO 70 II=I2,LE
      DE4(LL)=DABS(DE3(LNE)-DE3(II))
   70 LL=LL+1
   46 CONTINUE
      IF(IS(J)) 20,20,44
   44 CONTINUE
      DO 71 L1=LGF,K1
      DE4(LL)=DABS(DE2(L1)-DE5(L1))
   71 LL=LL+1
   20 CONTINUE
      NFD=LL-1
C
```

```
C    CALCULATE R MATRIX WHICH IS CALC - OBS DIFFS
C
      DO 25 I=1,NFD
   25 R(I)=DE4(I)-DEOB(I)
C
C    SET UP DERIVATIVE MATRIX BY VARYING EACH PARAMETER SEPERATELY
C    TO OBTAIN CHANGE IN FREQS.  AND PROCEDURE IS SAME AS IN
C    DETERMINING R MATRIX.
C
      DO 50 J=1,NP
      DO 51 K=1,13
   51 PARN(K)=PAR(K)
      PARN(J)=PAR(J)+DEN(J)
      DO 61 K=1,3
      K4=K+4
      K7=K+7
      K10=K+10
      G1(1,K)=PARN(K10)
      B(1,K)=PARN(K4)
   61 B(2,K)=PARN(K7)
      CALL TWSF(CC,HH,ACOS,DECOS,GCOS,GECOS,PARN)
      KK=1
      LL=1
      L=1
      JJ=1
      DO 52 N=1,NFLP
      DO 53 K=1,3
   53 UH(K)=UHM(N,K)
      CALL SSESR(NN,ACOS,GCOS,B,G1,UH,H,DE,GEF,FINT,IC)
      CALL SSESR(NN,DECOS,GECOS,B,G1,UH,H,DEE,GEFE,FINT,IC)
      NF=NFR(N)
      DO 54 K=1,NF
      MM=IFS(N,K)
      DE1(L)=DE(MM)
   54 L=L+1
      NFE=NFRE(N)
      DO 56 K=1,NFE
      MM=IFE(N,K)
      DE3(JJ)=DEE(MM)
   56 JJ=JJ+1
      LG=LGR(N)
      DO 57 K=1,LG
      MM=IFM(N,K)
      KL=IFN(N,K)
      DE2(KK)=DE(MM)
      DE5(KK)=DEE(KL)
   57 KK=KK+1
      LNE=JJ-NFE
      LE=JJ-1
      LGF=KK-LG
      K1=KK-1
      LNF=L-NF
      LM=L-1
      I1=LNF+1
      I2=LNE+1
      IF(IT(N)) 215,215,216
  216 CONTINUE
      DO 710 K=I1,LM
      DE6(LL)=DABS(DE1(LNF)-DE1(K))
  710 LL=LL+1
  215 CONTINUE
      IF(IR(N)) 58,58,210
  210 CONTINUE
      DO 220 II=I2,LE
      DE6(LL)=DABS(DE3(LNE)-DE3(II))
  220 LL=LL+1
   58 CONTINUE
      IF(IS(N)) 52,52,224
  224 CONTINUE
      DO 225 L1=LGF,K1
      DE6(LL)=DABS(DE2(L1)-DE5(L1))
  225 LL=LL+1
   52 CONTINUE
C
C    NFD = NO. OF DIFFS TAKEN
C
      NFD=LL-1
      DO 50 K=1,NFD
   50 DT(J,K)=(DE6(K)-DE4(K))/DEN(J)
C
C    THE DERIVATIVE MATRIX (DT) HAS BEEN FORMED.  ENTER BSTFT
C    FOR LEAST SQUARES FIT
C
      CALL BSTFT(DT,R,DEL,NP,NFD)
      DO 55 K=1,NP
   55 PAR(K)=PAR(K)-DEL(K)
   60 WRITE(6,116)(PAR(N),N=1,NP)
C
C    PAR CONTAINS NEW PARAMETERS FOR NEXT ITERATION
C
```

```
      GO TO 1
   15 FORMAT(6A8/3A8/3A8)
  100 FORMAT(I5,F10.5,13F5.0)
  101 FORMAT (9F7.5)
  102 FORMAT (3F7.3)
  103 FORMAT (3F7.5)
  104 FORMAT(1X,//' DIRECTION COSINES FOR THE ''A'' PRINCIPAL VALUES'//)
  105 FORMAT (1X,9F12.7)
  106 FORMAT (1X,//' COUPLING CONSTANTS'//)
  107 FORMAT (1X,3F10.5)
  108 FORMAT (1X,/////' DIRECTION COSINES FOR H',//(3F12.7)//)
  109 FORMAT (1X,' TRANSITION FREQUENCIES',//(10F11.5)//)
  110 FORMAT (1X,' TRANSITION INTENSITIES',//(10F11.5)//)
  111 FORMAT ((1H1,'NUCLEAR ZEEMAN FREQUENCY = 'F11.5)//)
  112 FORMAT (//' TRANSITIONS, IN GAUSS FROM CENTER, ASSUMING G = 2.0023
     1',//(10F11.5)//)
  113 FORMAT(8F10.5)
  114 FORMAT(3F10.6/3F10.6)
  115 FORMAT(1X,//' REFERENCE PARAMETERS',//(10F11.6)//)
  116 FORMAT(1X,//' NEW PARAMETERS',//(11F11.5)//)
  117 FORMAT(16I5)
  118 FORMAT(1X,//' DIFFS PER FIELD ORIENTATION = 'I5,' NO. FIELD ORIENT
     1ATIONS = 'I5//)
  119 FORMAT(1X,//' G EFFECTIVE = 'F10.5,3X,' G EFFECTIVE,EQIV.SITE = ',
     1F10.5//)
  120 FORMAT(1X,//' ERRORS, CALC - OBS FREQS',//(10F11.5)//)
  121 FORMAT(1X,//(10F11.5)//)
  122 FORMAT(1X,//' DT(I,J): CHANGE IN PARAMETER PER CHANGE IN POINT',/)
  123 FORMAT(1X,//' CALCULATED DIFFERENCES',//(10F11.5)//)
  124 FORMAT(1X,//' THE PRINCIPAL VALUES OF THE G TENSOR ARE'//(3F10.5))
  125 FORMAT(1X,//' DIRECTION COSINES FOR THE ''G'' PRINCIPAL VALUES'//(
     110F11.5)//)
  126 FORMAT(24I3)
  127 FORMAT(1X,/' FOR THE EQUIVALENT SITE'//)
  128 FORMAT(24F3.0)
  129 FORMAT(4X,/' TOTAL POINTS OBSERVED = ',I5,//)
      END
C
C
C
C
      SUBROUTINE SPEC(ITITLE,D,FINT,IC,MODCUR,YI)
C
C   SPEC DRAWS PREDICTED SPECTRA USING A LORENTZIAN DIST'N
C   PLACES 4 SPECTRA ON A GRAPH.  MAX OF 15 GRAPHS.
```

```
C
      DIMENSION F(900),D(32),FINT(32)
     1,W(900)
      REAL*8 ITITLE(12)
      W(1)=0.000
      DO 16 I=1,899
      IX=I+1
   16 W(IX)=W(I)+.100
      DO 71 I=1,900
   71 F(I)=0.0
      ICT=IC*2
      DO 120 I=1,ICT
  120 D(I)=D(I)+37.5
C
C   WI = LINEWIDTH
C
      WI=2.1
      T2=2/(1.73502*WI)
      DO 72 I=1,900
      DO 72 J=1,ICT
   72 F(I)=F(I)-2*(W(I)-D(J))*T2*FINT(J)/(1+(T2*(W(I)-D(J)))**2)**2
      DO 110 I=1,900
      W(I)=.877*W(I)
  110 F(I)=-.025*F(I)+YI
      CALL DRAW(900,F,W,MODCUR,0,LABEL,ITITLE,2.0E-02,6.,0,1,0,2,9,15,0,
     1LAST)
      WRITE(6,80) LAST
   80 FORMAT(//' GRAPH OPERATION'/F10.5)
      RETURN
      END
C
C
C
C
      SUBROUTINE BSTFT(DT,R,DEL,IR,IS)
C
C   THIS PROGRAM MULTIPLIES THE FOLLOWING MATRICIES - DT TIMES D,
C   INVERTED, TIMES DT, TIMES R.
C   DT IS THE TRANSPOSE OF THE DERIVATIVE MATRIX.
C   THE LEAST SQUARES FIT PERFORMED GIVES BEST CHANGES TO BE MADE
C   IN PARAMETERS.
C   UNCERTAINTIES FOR EACH PARAMETER ARE CALC.
C
      IMPLICIT REAL*8(A-H,O-Z)
      DIMENSION DT(13,250),R(250),DEL(13)
     1,DPI(13,13),U(13,13),DX(13),DPS(13,13)
      PRINT 104, (IR,IS)
      PRINT 109
      DO 20 I = 1,IR
      PRINT 101, (DT(I,J), J = 1,IS)
   20 PRINT 105
      PRINT 105
      PRINT 110
      PRINT 102, (R(I), I = 1,IS)
      PRINT 105
      CALL FIT(IR,IS,DT,R,DEL,DPI,U,DPS)
      RSUM = 0.0
      DO 30 I = 1,IS
   30 RSUM = RSUM+R(I)**2
      PRINT 106, (RSUM)
      AR=IS-1
      RSUM=RSUM/AR
      SD=DSQRT(RSUM)
      WRITE(6,112) SD
      PRINT 105
      DO 35 I = 1,IS
      DO 35 J = 1,IR
   35 R(I) = R(I)-DT(J,I)*DEL(J)
      PRINT 111
      PRINT 102, (R(I), I = 1,IS)
      RSUM = 0.0
      DO 40 I = 1,IS
   40 RSUM = RSUM+R(I)**2
      PRINT 107, (RSUM)
      RSUM=RSUM/AR
      SD=DSQRT(RSUM)
      WRITE(6,113) SD
      DO 45 I=1,IR
      DSX=RSUM*DPI(I,I)
   45 DX(I)=DSQRT(DSX)
      PRINT 114
      PRINT 103, (DX(I),I=1,IR)
      DO 50 I=1,IR
      DO 50 J=1,IR
   50 U(J,I)=U(I,J)
      PRINT 105
      PRINT 108
      PRINT 103, (DEL(I), I = 1,IR)
  100 FORMAT (3I5)
  101 FORMAT (10F8.2)
```

```
 102 FORMAT (10F8.4)
 103 FORMAT (1H , 5E20.8)
 104 FORMAT (//' NUMBER OF PARAMETERS = 'I2,'   NUMBER OF POINTS = 'I3,
    1//)
 105 FORMAT (1H )
 106 FORMAT (37H ORIGINAL SUM OF SQUARES OF ERRORS = ,E15.8)
 107 FORMAT (32H NEW SUM OF SQUARES OF ERRORS = ,E15.8)
 108 FORMAT (41H ADD TO ORIGINAL PARAMETERS THE FOLLOWING)
 109 FORMAT ('  THE TRANSPOSE OF THE DERIVATIVE MATRIX IS',//)
 110 FORMAT (//,'  THE ORIGINAL ERRORS BETWEEN CALCULATED AND OBSERVED
    1ARE',//)
 111 FORMAT (//,'  THE ERRORS AFTER THE ITERATION ARE',//)
 112 FORMAT(/,' ORIGINAL STD DEVIATION = ',E15.8)
 113 FORMAT(/,' NEW STD DEVIATION = ',E15.8)
 114 FORMAT(//' THE UNCERTAINTIES IN THE PARAMETERS ARE',//)
      RETURN
      END
C
C
C
C
      SUBROUTINE FIT(IR,IS,DT,R,DEL,DPI,U,DPS)
C
C   IR IS NUMBER OF VARIABLES
C   IS IS NUMBER OF OBSERVED POINTS
C   DT IS THE DERIVATIVE MATRIX, IR ROWS, IS COLUMNS
C   R IS THE DIFF MATRIX, COLUMN, WITH IS ELEMENTS
C   DEL IS THE VALUE TO BE ADDED TO EACH VARIABLE, A COLUMN MATRIX
C   WITH IR ELEMENTS
C   THIS PROGRAM SUPPLEMENTS BSTFT AND PERFORMS THE MATRIX
C   MULTIPLICATIONS INDICATED IN BSTFT.
C
      IMPLICIT REAL*8(A-H,O-Z)
      DIMENSION DT(13,250),DEL(13),R(250),DTR(13),DP(13,13),DPI(13,13)
     2,DPS(13,13),U(13,13)
      DO 30 I = 1,IR
      DTR(I) = 0.0
      DO 30 J = 1,IS
   30 DTR(I) = DTR(I)+DT(I,J)*R(J)
      DO 40 I = 1,IR
      DO 40 J = 1,IR
      DP(I,J) = 0.0
      DO 40 K = 1,IS
   40 DP(I,J) = DP(I,J)+DT(I,K)*DT(J,K)
      DO 60 I=1,IR
      DO 60 J=1,IR
   60 DPS(I,J)=DP(I,J)
      CALL HDIAG(DPS,U,0,IR,NR)
      WRITE(6,112)(DPS(I,I),I=1,IR)
  112 FORMAT(1X,//' EIGENVALUES',//(10E12.5)//)
      WRITE(6,113)((U(I,J),J=1,IR),I=1,IR)
  113 FORMAT(1X,//' EIGENVECTORS',//(10F11.5)//)
      CALL GAUSS3(IR,1.00E-30,DP,DPI,ITEST)
      PRINT 110
      DO 55 I=1,IR
   55 PRINT 111,(DPI(I,J),J=1,IR)
  110 FORMAT(//' THE INVERSE OF THE DERIVATIVE MATRIX IS'//)
  111 FORMAT(10E11.3)
      IF(ITEST-1) 42,45,42
   42 PRINT 100
   45 DO 50 I = 1,IR
      DEL(I) = 0.0
      DO 50 J = 1,IR
   50 DEL(I) = DEL(I)+DPI(I,J)*DTR(J)
  100 FORMAT (16H MATRIX SINGULAR)
      RETURN
      END
C
C
C
C
      SUBROUTINE HDIAG(H,U,IEGEN,N,NR)
C
C THIS ROUTINE DIAGONALIZES H AND DETERMINES THE ROW EIGENVECTORS U
C THIS VERSION OF HDIAG WORKS ON THE FULL MATRIX, NOT JUST THE UPPER HALF.
C
      IMPLICIT REAL*8(A-H,O-Z)
      DIMENSION H(13,13), U(13,13), X(13), IQ(13)
      M = 1
      FN = N
      DO 10 I = M,N
      DO 10 J = M,N
   10 U(I,J) = 0.0
      DO 12 I = M,N
   12 U(I,I) = 1.0
   15 NR = 0
      SUM = 0.0
      DO 16 I = M,N
      DO 16 J = I,N
   16 SUM = SUM+H(I,J)**2
```

```
      SUM=DSQRT(SUM/(FN*FN))
      SUM = SUM*1.00E-08
   19 N1 = N-1
      N2 = N-2
   20 IF(N2) 1000,40,22
   22 DO 39 I = M,N2
      K = I+1
      XMAX = 0.0
      DO 25 J = K,N
      IF(DABS(H(I,J))-XMAX) 25,25,23
   23 XMAX=DABS(H(I,J))
      IQS = J
   25 CONTINUE
      IQ(I) = IQS
   39 X(I) = XMAX
   40 X(N1) = H(N1,N)
      IQ(N1) = N
   41 ZMAX = 0.0
      DO 43 I = M,N1
      IF(X(I)-ZMAX) 43,43,42
   42 ZMAX = X(I)
      IPIV = I
   43 CONTINUE
      JPIV = IQ(IPIV)
      IF(ZMAX-SUM) 1000,1000,150
  150 NR = NR+1
      Z1 = H(IPIV,IPIV)
      Z2 = H(JPIV,JPIV)
      Z3 = H(IPIV,JPIV)
      Z4 = 4.0*Z3**2
      Z5 = (Z1-Z2)**2
      Z6 = (Z2-Z1)*Z3
      IF(DABS(Z5/Z4)-10.0) 50,52,52
   50 SINSQ=0.5-0.5*DSQRT(Z5/(Z4+Z5))
      GO TO 55
   52 TC2 = Z4/Z5
      SINSQ = 0.25*TC2*(1.0-0.75*TC2*(1.0-0.833333333333*TC2*(1.0-0.875*
     1TC2*(1.0-0.9*TC2*(1.0-0.91666666667*TC2*(1.0-0.928571428 57*TC2*
     2(1.0-0.9375*TC2))))))
   55 COSSQ = 1.0-SINSQ
      COSINE=DSQRT(COSSQ)
      SINE=DSQRT(SINSQ)
      IF(Z6) 90,90,85
   85 SINE = -SINE
   90 SCH = 2.0*SINE*COSINE*Z3
```

```
      HIPIP = COSSQ*Z1+SINSQ*Z2+SCH
      HJPJP = COSSQ*Z2+SINSQ*Z1-SCH
      DO 100 I = M,N
      HIPI = H(IPIV,I)
      HJPI = H(JPIV,I)
      H(IPIV,I) = COSINE*HIPI+SINE*HJPI
      H(JPIV,I) = -SINE*HIPI+COSINE*HJPI
      H(I,IPIV) = H(IPIV,I)
  100 H(I,JPIV) = H(JPIV,I)
      H(IPIV,IPIV) = HIPIP
      H(JPIV,JPIV) = HJPJP
      H(IPIV,JPIV) = 0.0
      H(JPIV,IPIV) = 0.0
  200 IDF = JPIV-IPIV
      DO 220 INT = IPIV,JPIV,IDF
      IPM = INT+1
      IF(IPM-N) 220,201,201
  201 XMAX = 0.0
      DO 210 I = IPM,N
      IF(DABS(H(INT,I))-XMAX) 210,210,205
  205 XMAX=DABS(H(INT,I))
      IQS = I
  210 CONTINUE
  219 X(INT) = XMAX
      IQ(INT) = IQS
  220 CONTINUE
      DO 260 INT = IPIV,JPIV,IDF
      IPM = INT-1
      IF(IPM) 260,260,229
  229 DO 250 I = M,IPM
      IF(IQ(I)-INT) 240,230,240
  230 K = I+1
      XMAX=DABS(H(I,INT))
      IQS = INT
      DO 238 J = K,N
      IF(DABS(H(I,J))-XMAX) 238,238,236
  236 XMAX=DABS(H(I,J))
      IQS = J
  238 CONTINUE
      X(I) = XMAX
      IQ(I) = IQS
      GO TO 250
  240 IF(DABS(H(I,INT))-X(I)) 250,250,245
  245 X(I)=DABS(H(I,INT))
      IQ(I) = INT
  250 CONTINUE
  260 CONTINUE
      IF(IEGEN) 41,500,41
  500 DO 550 I = M,N
      UIPI = U(IPIV,I)
      UJPI = U(JPIV,I)
      U(IPIV,I) = COSINE*UIPI+SINE*UJPI
  550 U(JPIV,I) = -SINE*UIPI+COSINE*UJPI
  555 GO TO 41
 1000 N1 = N-1
      DO 655 J = 1,N1
      XMAX = H(J,J)
      JQ = J
      J1 = J+1
      DO 645 I = J1,N
      IF(H(I,I)-XMAX) 645,645,643
  643 XMAX = H(I,I)
      JQ = I
  645 CONTINUE
      TEMP = H(J,J)
      H(J,J) = H(JQ,JQ)
      H(JQ,JQ) = TEMP
      DO 650 I = M,N
      TEMP = U(J,I)
      U(J,I) = U(JQ,I)
  650 U(JQ,I) = TEMP
  655 CONTINUE
      RETURN
      END
C
C
C
C
      SUBROUTINE   GAUSS3(N,EP,A,X,KER)
      IMPLICIT REAL*8(A-H,O-Z)
C
C    THIS PROGRAM INVERTS A MATRIX.
C
      DIMENSION A(13,13),X(13,13)
      DO 1 I=1,N
      DO 1 J=1,N
    1 X(I,J)=0.0
      DO 2 K=1,N
    2 X(K,K)=1.0
   10 DO 34 L=1,N
```

```
      KP=0
      Z=0.0
      DO 12 K=L,N
      IF(Z-DABS(A(K,L))) 11,12,12
   11 Z=DABS(A(K,L))
      KP=K
   12 CONTINUE
      IF(L-KP)13,20,20
   13 DO 14 J=L,N
      Z=A(L,J)
      A(L,J)=A(KP,J)
   14 A(KP,J)=Z
      DO 15 J=1,N
      Z=X(L,J)
      X(L,J)=X(KP,J)
   15 X(KP,J)=Z
   20 IF(DABS(A(L,L))-EP) 50,50,30
   30 IF(L-N)31,34,34
   31 LP1=L+1
      DO 36 K=LP1,N
      IF(A(K,L))32,36,32
   32 RATIO=A(K,L)/A(L,L)
      DO 33 J=LP1,N
   33 A(K,J)=A(K,J)-RATIO*A(L,J)
      DO 35 J=1,N
   35 X(K,J)=X(K,J)-RATIO*X(L,J)
   36 CONTINUE
   34 CONTINUE
   40 DO 43 I=1,N
      II=N+1-I
      DO 43 J=1,N
      S=0.0
      IF(II-N)41,43,43
   41 IIP1=II+1
      DO 42 K=IIP1,N
   42 S=S+A(II,K)*X(K,J)
   43 X(II,J)=(X(II,J)-S)/A(II,II)
      KER=1
      RETURN
   50 KER=2
      RETURN
      END
C
C
C
```

```
C
      SUBROUTINE SSESR(NN,ACOS,GCOS,A,G,UH,H,DE,GEF,FINT,IC)
C
C    THIS PROGRAM CALCS FREQS AND INTS. FOR ORIENTED RADICALS.
C    ALSO CALC. EFFECTIVE G VALUE (GEF) AND COMPUTES THE CHEMICAL
C    SHIFT OF EACH SITE RELATIVE TO EACH OTHER.
C   NN IS THE NUMBER OF NUCLEI WITH SPIN = .5
C   ACOS & GCOS ARE THE DIRECTION COSINE MATRICES FOR A AND G TENSORS.
C   ELEMENT I,J,K RELATES THE COMPONENT  FOR ATOM I OF THE J-TH PRINCIPAL
C   AXIS ALONG THE K-TH CRYSTAL AXIS
C   A(I,J) IS THE J-TH PRINCIPAL VALUE FOR THE I-TH ATOM
C   UH(I) IS THE I-TH COMPONENT OF THE UNIT VECTOR POINTING ALONG THE
C      DIRECTION OF THE MAGNETIC FIELD
C   DE IS THE ARRAY OF TRANSITION FREQUENCIES CALCULATED
C   FINT IS THE CORRESPONDING ARRAY OF INTENSITIES
C   IC IS THE NUMBER OF TRANSITIONS CALCULATED
C
      IMPLICIT REAL*8(A-H,O-Z)
      DIMENSION ACOS(2,3,3),A(2,3),UH(3),DE(16),FINT(16),
     1HV(2,3),HVP(2,2,3),CE(10),HCOS(2,3),ABH(2,2),S(2),IQ(20),
     2GCOS(2,3,3),G(2,3),PCOS(2,3)
      S(1) = 1.0
      S(2)=-1.0
      DO 10 I=1,NN
      DO 10 J=1,3
      HCOS(I,J) = 0.0
      PCOS(I,J)=0.0
      DO 10 K=1,3
      PCOS(I,J)=PCOS(I,J)+UH(K)*GCOS(I,J,K)
   10 HCOS(I,J)=HCOS(I,J)+UH(K)*ACOS(I,J,K)
      DO 15 I = 1,NN
      DO 15 J = 1,3
   15 HV(I,J) = 0.0
      DO 20 I = 1,NN
      DO 20 J = 1,3
      CAS = HCOS(I,J)*A(I,J)
      DO 20 K = 1,3
   20 HV(I,K) = HV(I,K) + CAS*ACOS(I,J,K)
      I=1
      GEF=0.0
      DO 32 K=1,3
   32 GEF=GEF+(PCOS(I,K)*G(I,K))**2
      GEF=DSQRT(GEF)
      DO 30 I = 1,NN
      DO 30 J = 1,2
      DO 30 K = 1,3
   30 HVP(I,J,K) = H*UH(K)-0.5*S(J)*HV(I,K)
      DO 40 I = 1,NN
      DO 40 J = 1,2
      ABH(I,J) = 0.0
      DO 35 K = 1,3
   35 ABH(I,J) = ABH(I,J) + HVP(I,J,K)**2
   40 ABH(I,J)=DSQRT(ABH(I,J))
      DO 50 I = 1,NN
      CE(I) = 0.0
      DO 45 J = 1,3
   45 CE(I) = CE(I) + HVP(I,1,J)*HVP(I,2,J)
   50 CE(I) = CE(I)/(ABH(I,1)*ABH(I,2))
      NN2 = 2*NN
      NNTT = 2**(2*NN)
      HNNT = 2**NN
      DO 55 I = 1,NN2
   55 IQ(I) = 1
      IC = 0
      DO 70 I = 1,NNTT
      IC = IC+1
      DE(IC) = 0.0
      FINT(IC) = 1.0
      DO 60 J = 1,NN
      J1 = IQ(J)
      J2 = IQ(NN+J)
      FINT(IC) = FINT(IC)*(1.0-S(J1)*S(J2)*CE(J))
   60 DE(IC) = DE(IC) + S(J1)*ABH(J,1) + S(J2)*ABH(J,2)
      DE(IC) = 0.5*DE(IC)
      FINT(IC) = FINT(IC)/HNNT
      J = 1
   64 IF(IQ(J)-2) 66,65,66
   65 IQ(J) = 1
      J = J+1
      GO TO 64
   66 IQ(J) = 2
   70 CONTINUE
  100 FORMAT (1H ,10F11.5)
      DO 200 I=1,IC
  200 DE(I)=(6447.3619/GEF)-3220. + DE(I)/(1.39963*GEF)
      RETURN
      END
C
C
C
```

```
C
      SUBROUTINE TWSF(A,B,ACOS,DECOS,GCOS,GECOS,PAR)
C
C    THIS PROGRAM SETS UP DIRECTION COSINES FOR THE PLANAR
C    RADICAL IN THE CRYSTAL AXIS SYSTEM.  THEN THE ANGLES FOR
C    TWIST, WAG, FLAP, AND HCH ANGLE ARE USED TO RE-ORIENT THE
C    RADICAL.  THE DC'S ARE CHANGED FOR A CHANGE IN ANY OF THESE
C    PARAMETERS.
C    A(I) AND B(I) - KNOWN VECTORS IN THE ORIENTED RADICAL.
C
      IMPLICIT REAL*8(A-H,O-Z)
      DIMENSION A(3),B(3),Y(3),CH1(3),CH2(3),X1(3),X2(3),ACOS(2,3,3)
     1,PAR(13),DECOS(2,3,3),GECOS(2,3,3),GCOS(2,3,3)
      CALL CROSSP(A,B,Y)
      HHCH=PAR(4)/2.0
      CANG=90.0-HHCH
      HHCH=HHCH*3.1416/180.0
      CANG=CANG*3.1416/180.0
      D=DCOS(HHCH)
      E=DCOS(CANG)
      DO 10 I=1,3
      CH1(I)=D*A(I)+E*B(I)
   10 CH2(I)=D*A(I)-E*B(I)
      CALL CROSSP(Y,CH1,X1)
      CALL CROSSP(Y,CH2,X2)
      DO 15 I=1,2
      DO 15 J=1,3
      DO 15 K=1,3
      GECOS(I,J,K)=0.0
   15 GCOS(I,J,K)=0.0
      J=1
      K=2
      L=3
      DO 20 M=1,2
      DO 20 I=1,3
      GO TO (30,40),M
   30 ACOS(M,J,I)=CH1(I)
      ACOS(M,K,I)=Y(I)
      ACOS(M,L,I)=X1(I)
      GCOS(M,J,I)=A(I)
      GCOS(M,K,I)=B(I)
      GCOS(M,L,I)=Y(I)
      GO TO 20
   40 ACOS(M,J,I)=CH2(I)
      ACOS(M,K,I)=Y(I)
      ACOS(M,L,I)=X2(I)
   20 CONTINUE
      CALL AXR(A,ACOS,PAR(1))
      CALL AXR(Y,ACOS,PAR(2))
      CALL AXR(B,ACOS,PAR(3))
      CALL AXR(A,GCOS,PAR(1))
      CALL AXR(Y,GCOS,PAR(2))
      CALL AXR(B,GCOS,PAR(3))
      DO 50 I=1,2
      DO 50 J=1,3
      DO 50 K=1,3
      DECOS(I,J,K)=ACOS(I,J,K)
   50 GECOS(I,J,K)=GCOS(I,J,K)
      Y(1)=0.0
      Y(2)=1.0
      Y(3)=0.0
      CALL AXR(Y,GECOS,180.)
      CALL AXR(Y,DECOS,180.)
      RETURN
      END
C
C
C
C

      SUBROUTINE CROSSP(A,B,C)
C
C   THIS PROGRAM CALCS THE CROSS PRODUCT BETWEEN TWO VECTORS.
C
      IMPLICIT REAL*8(A-H,O-Z)
      DIMENSION A(3),B(3),C(3)
      C(1)=A(2)*B(3)-A(3)*B(2)
      C(2)=A(3)*B(1)-A(1)*B(3)
      C(3)=A(1)*B(2)-A(2)*B(1)
      RETURN
      END
C
C
C
C

      SUBROUTINE AXR(A,ACOS,ANGLE)
C
C   THIS PROGRAM CHANGES THE DIRECTION COSINES FOR EACH TENSOR FOR A
C   CHANGE IN ANY PARAMETER (ANGLE)
C
      IMPLICIT REAL*8(A-H,O-Z)
      DIMENSION A(3),ACOS(2,3,3),ROTM(3,3),ROTMT(3,3),AR(3,3),S(3,3)
     1,S1(3,3),DCOS1(3,3),DCOS2(3,3),DCOS3(3,3),DCOS4(3,3)
      E=DSQRT(1.0-A(3)**2)
      DO 10 I=1,3
      DO 10 J=1,3
   10 ROTM(I,J)=0.0
      ROTM(1,1)=A(2)/E
      ROTM(1,2)=-A(1)/E
      ROTM(2,1)=A(1)*A(3)/E
      ROTM(2,2)=A(2)*A(3)/E
      ROTM(2,3)=-E
      ROTM(3,1)=A(1)
      ROTM(3,2)=A(2)
      ROTM(3,3)=A(3)
      CALL GMTRA(ROTM,ROTMT,3,3)
      ANGN=ANGLE*3.14159265/180.
      F=DCOS(ANGN)
      G=DSIN(ANGN)
      DO 20 I=1,3
      DO 20 J=1,3
   20 AR(I,J)=0.0
      AR(1,1)=F
      AR(1,2)=G
      AR(2,1)=-G
      AR(2,2)=F
      AR(3,3)=1.0
      CALL GMPRD(AR,ROTM,S,3,3,3)
      CALL GMPRD(ROTMT,S,S1,3,3,3)
      I=1
      L=2
      DO 30 J=1,3
      DO 30 K=1,3
      DCOS1(K,J)=ACOS(I,J,K)
   30 DCOS2(K,J)=ACOS(L,J,K)
      CALL GMPRD(S1,DCOS1,DCOS3,3,3,3)
      CALL GMPRD(S1,DCOS2,DCOS4,3,3,3)
      DO 40 J=1,3
      DO 40 K=1,3
      ACOS(I,J,K)=DCOS3(K,J)
   40 ACOS(L,J,K)=DCOS4(K,J)
      RETURN
      END
C
C
C
```

```
C
      SUBROUTINE GMTRA(A,R,N,M)
C
C   THIS PROGRAM WILL TRANSPOSE A GENERAL MATRIX.
C
      IMPLICIT REAL*8(A-H,O-Z)
      DIMENSION A(1),R(1)
      IR=0
      DO 10 I=1,N
      IJ=I-N
      DO 10 J=1,M
      IJ=IJ+N
      IR=IR+1
   10 R(IR)=A(IJ)
      RETURN
      END
C
C
C
C
      SUBROUTINE GMPRD(A,B,R,M,N,L)
C
C   THIS PROGRAM WILL CALC THE PRODUCT OF 2 MATRICES.
C
      IMPLICIT REAL*8(A-H,O-Z)
      DIMENSION A(1),B(1),R(1)
C
      IR=0
      IK=-M
      DO 10 K=1,L
      IK=IK+M
      DO 10 J=1,N
      IR=IR+1
      JI=J-N
      IB=IK
      R(IR)=0
      DO 10 I=1,M
      JI=JI+N
      IB=IB+1
   10 R(IR)=R(IR)+A(JI)*B(IB)
      RETURN
      END
C
C
C   A SAMPLE OF THE DATA IS AS FOLLOWS
```

```
C
C
   2    13.70   1.    1.    1.   1.    1.   1.    1.    1.   1.    1.    .0001.0
.675092    .455907    -.579999
.269381    .579567    .769115
0.0        0.0        0.0        120.       -29.       -61.       -91.        -2
-61.       -91.       2.0042     2.00353    2.00242
  1   2  2  3   1  2  2   3  1  2   2  3  1   2  2  3   1  2  2   3  1  2   2  3
  1   2  2  3   1  2  2   3  1  2   2  3  1   2  2  3   1  2  2   3  1  2   2  3
  1   2  2  3   1  2  2   3  1  2   2  3  1   2  2  3   1  2  2   3  1  2   2  3
0.0.04.08.120.0.04.08.120.0.04.08.120.0.04.08.120.0.04.08.120.0.04.08.12
0.0.04.08.120.0.04.08.120.0.04.08.120.0.04.08.120.0.04.08.120.0.04.08.12
0.0.04.08.120.0.04.08.120.0.04.08.120.0.04.08.120.0.04.08.120.0.04.08.12
  17    10      1
JOB OPTIM  CRAWFORD BOX 41
EPR SPECTRA
WI=2.1
    3     3     2    3     3    3     3    2     3     3    3     2    2     2
    2
    1     1     1    1     1    1     1    1     1     1    1     2    2     2
    2
    1     1     1    1     1    1     1    2     2     2    2     1    2     2
    2
    1     1     1    1     1    1     1    1     1     1    1     1    1     1
    1
    0     0     0    0     0    0     0    0     0     0    0     1    1     1
    1
    0     0     0    0     0    0     0    1     1     1    1     1    1     1
    1
0.0     0.0     1.0
  1  6 11
  1
  1
  1
29.78      10.34
.500    0.0     .86603
  1  6 11
  1
  1
  1
23.50      17.17
.70711 0.0      .70711
  1 16
  1
  1
  1
40.58
.86603 0.0    .50
  1  6 11
  1
  1
  1
17.7      24.09
.96592 0.0    .25882
  1  6 11
  1
  1
  1
18.12      26.07
1.0    0.0    0.0
  1  6 11
  1
  1
  1
20.96      26.61
0.0    1.0    0.0
  1  6 11
  1
  1
  1
18.50      28.62
.96592 .25882 0.0
  1  6
  1
 11 11
 16  1
19.39      15.49     29.21
.86603 .50000 0.0
  1  6 11
  1
 11  6
 16 16
18.31      31.75     12.87     26.31
.70711 .70711 0.0
  1  6 11
  1
 11  6
 16 16
17.58      32.69     11.23     26.34
.5000  .86603 0.0
```

DOCUMENT CONTROL DATA - R & D

(Security classification of title, body of abstract and indexing annotation must be entered when the overall report is classified)

1. ORIGINATING ACTIVITY *(Corporate author)* Naval Postgraduate School Monterey, California 93940	2a. REPORT SECURITY CLASSIFICATION Unclassified 2b. GROUP

3. REPORT TITLE

Electron Paramagnetic Resonance of the $\cdot CH_2CO_2^-$ Radical in Irradiated Zinc Acetate Dihydrate

4. DESCRIPTIVE NOTES *(Type of report and inclusive dates)*

Master of Science Thesis, June 1968

5. AUTHOR(S) *(First name, middle initial, last name)*

Leslie P. Crawford

6. REPORT DATE June 1968	7a. TOTAL NO. OF PAGES 110	7b. NO. OF REFS 34

8a. CONTRACT OR GRANT NO.	9a. ORIGINATOR'S REPORT NUMBER(S)
b. PROJECT NO.	
c.	9b. OTHER REPORT NO(S) *(Any other numbers that may be assigned this report)*
d.	

10. DISTRIBUTION STATEMENT

[redacted]

11. SUPPLEMENTARY NOTES	12. SPONSORING MILITARY ACTIVITY Naval Postgraduate School Monterey, California 93940

13. ABSTRACT

An electron paramagnetic resonance study of the $\cdot CH_2CO_2^-$ radical in irradiated zinc acetate dihydrate has been made. The configuration of the radical in the crystalline lattice has been determined as nearly planar using a least squares fit. The HCH angle was found to be $116.9^\circ \pm .3^\circ$. The principal elements of the α-proton hyperfine tensors were calculated to be: $-26.80 \pm .74$, $-59.59 \pm .44$, $-92.15 \pm .31$ for H_1; $-26.41 \pm .99$, $-58.98 \pm .45$, $-92.78 \pm .20$ for H_2. Three principal values of the g tensor were selected for the best least squares fit: 2.00242, 2.00353, 2.0042. By experiment and an MO calculation the radical has been shown to be a π-electron radical with the unpaired electron localized on the α-carbon. Satellite lines were observed and interpreted as possible "spin-flip" transitions. A temperature dependence of the coupling constants for the 2 protons was discovered from spectra taken at room temperature and at $133^\circ K$. Single crystals of $Zn(CH_2DCO_2)_2 \cdot 2H_2O$ were irradiated and an analysis of the spectra showed that the barrier to formation of the radical was the breaking of the C-H bond on the undamaged acetate ion.

14. KEY WORDS	LINK A		LINK B		LINK C	
	ROLE	WT	ROLE	WT	ROLE	WT
ESR						
anisotropic						
radical orientation						
axis systems						
irradiation damage						
zinc acetate						
least squares						
parameter						
isotope effect						
spin density						
electron paramagnetic resonance						
electron spin resonance						
radiation damage						
free radical						
single crystal						

[redacted]

[redacted]

thesC83
DUDLEY KNOX LIBRARY
3 2768 00422014 5
DUDLEY KNOX LIBRARY